UNIVERSITY OF VAASA

FACULTY OF TECHNOLOGY

ENERGY TECHNOLOGY

Ilkka-Matti Kattilakoski

BI-DIRECTIONAL DISTRIBUTED THERMAL RESPONSE TEST

Supervisor Erkki Hiltunen

Instructor Tapio Syrjälä

Contents

UNIVERSITY OF VAASA
Faculty of technology
Author: Ilkka-Matti Kattilakoski
Topic of the thesis: Bi-Directional Distributed Thermal Response Test
Supervisor: Erkki Hiltunen
Instructor: Tapio Syrjälä
Degree: Master of Science in Technology
Degree programme: Degree Programme in Electrical and Energy Engineering
Major: Energy Technology
Year of entering university: 2013
Year of completing thesis: 2017 **Pages:** 60

ABSTRACT:

The research problem is to perform a bi-directional distributed thermal response test (DTRT) and to describe what is occurring. With bi-directional is meant a heating and cooling test. Those, in addition to distributed temperature sensing (DTS) are useful for collecting information on groundwater flow in and around a borehole heat exchanger (BHE). An estimate on convective heat transfer is important if the bedrock is to be used as a heat store.

The thermal response test (TRT) procedure was described, along with some of its history. Additionally, heat pump-, borehole heat storage- and DTS technologies were elucidated.

A heating and cooling test with DTS was executed successfully. Subject of the experiment was a 122-meter deep BHE in Gerby, Vaasa.

The undisturbed ground temperature was determined by circulating the heat carrier fluid without heating. It was measured with Pt-100 sensors and DTS. The measured values were slightly higher during daytime and settled back in the evening. Calculated borehole thermal resistance was around the range typical of water-filled BHEs. It seemed to fluctuate over time to some extent, which was probably due to power quality variations.

No anomalies were found in the temperature distribution. Calculated effective thermal conductivity however suggests the presence of a groundwater flow. Ground layer atop the rock was significantly affected by outdoor temperature. The most probable explanation was that the rock was not fractured and horizontal groundwater flow was limited to the thin ground layer. The test was the first of its kind and its results shall remain as reference for future experiments.

KEYWORDS: Geoenergy, thermal response test, distributed temperature sensing, thermal energy storage

VAASAN YLIOPISTO
Teknillinen tiedekunta
Tekijä: Ilkka-Matti Kattilakoski
Diplomityön nimi: Bi-Directional Distributed Thermal Response Test
Valvoja: Erkki Hiltunen
Ohjaaja: Tapio Syrjälä
Tutkinto: Diplomi-insinööri
Koulutusohjelma: Sähkö- ja energiatekniikan koulutusohjelma
Suunta: Energiatekniikka
Opintojen aloitusvuosi: 2013
Diplomityön valmistumisvuosi: 2017 **Sivumäärä:** 60

TIIVISTELMÄ:

Tutkimusongelma on suorittaa kaksisuuntainen hajautettu terminen vastetesti ja kuvata kokonaisuus. Kaksisuuntaisuudella tarkoitetaan lämmitys- ja kylmennystestiä. Se, ja hajautettu lämpötilan mittaus ovat hyödyllisiä eritoten keräämään tietoa pohjavesivirtauksista lämpökaivon välittömässä läheisyydessä. Arvio konvektiivisesta lämmönsiirrosta on tärkeä, jos kalliota käytetään lämpövarastona.

Kuvattiin terminen vastetesti, sen historiaa, lämpöpumpputekniikka, lämpövarastotekniikka ja hajautettu lämpötilan mittaustekniikka.

Suoritettiin kaksisuuntainen terminen vastetesti hajautetulla lämpötilan mittauksella onnistuneesti. Kohteena oli 122 metriä syvä lämpökaivo Vaasan Gerbyssä.

Kallion alkulämpötila mitattiin hajautetusti ja Pt-100 antureilla kierrättämällä lämmönkeruunestettä ilman lämmitystä. Mitatut arvot kohosivat vähän päiväsaikaan ja tasaantuivat taas illaksi. Porakaivon lämpövastuksen laskettiin olevan suuruusluokaltaan tyypillinen vedentäyteisille kaivoille. Se näytti vaihtelevan vähän ajan myötä, mikä johtui luultavimmin virransyötön pienistä epätasaisuuksista.

Poikkeamia lämpötilajakaumassa ei löytynyt. Laskettu lämmönjohtavuus viittaa kuitenkin pohjavesivirtausten läsnäoloon. Pintamaakerrokseen vaikutti suuresti ulkolämpötilavaihtelut. Todettiin todennäköisimmäksi selitykseksi, että kalliossa ei ole halkeamia ja sivusuuntainen pohjavesivirtaus sijaitsee ohuessa maakerroksessa. Tämä oli laatuaan ensimmäinen testi, jonka tulokset jäävät referenssiksi tuleville kokeille.

AVAINSANAT: Geoenergia, terminen vastetesti, hajautettu lämpötilan mittaus, lämpövarasto

1. INTRODUCTION

Low enthalpy heat, such as that residing in the bedrock, can be utilized for the heating of buildings with heat pumps. A thermal response test (TRT) is used to measure thermal properties of the ground. This is mainly done for the purpose of calculating optimal dimensioning of ground/bedrock heating systems. The procedure is reasonably well established. It has been used in Sweden since the nineties and since then in many other countries.

There are two meaningful directions to develop the TRT. One is to make it cheaper while still retaining sufficient quality. Another is to make it better and more accurate. This thesis has to do with the latter.

Sometimes strong groundwater presence makes interpretation of the TRT result difficult. In bigger heating systems with multiple boreholes, there may be need for a more accurate awareness of groundwater properties. This is especially true if the ground is actively regenerated. Such technology is called borehole thermal energy storage (BTES). This means pumping warm heat exchanger liquid through cold rock to transfer heat to the rock, for the purpose of extracting such heat later. Typically, bedrock tends to have a high heat capacity and somewhat low conductivity.

Underground thermal energy storage (UTES) in general can be a significant contributor to reaching greenhouse emission goals, as it has great potential for improving energy efficiency of the heating of buildings.

In environments with groundwater presence, results that are more accurate may be obtained by performing a cooling test instead of the more convenient heating test. This is due to the heating induced convection. Then again, prolonged cooling may cause water to turn to ice, which releases heat, affecting results.

One way to acquire information about groundwater properties is a vertical temperature profile of the borehole. This can be accomplished with the use of distributed temperature sensing (DTS) technology.

In this work a combined heating and cooling test has been performed, while measuring the temperature profile with DTS. This has been the first of such tests with more to come. At the University of Vaasa there is also research going on about asphalt- and sediment heat.

2. GEOENERGY

Geothermal energy consists of all energy sources originating from below the ground. These include heat originating from the Earth's core, volcanic phenomena and heat from decaying long-lived radioactive isotopes such as U^{238}, U^{235}, Th^{232} and K^{40}. These isotopes can be found in the upper crust. The earth is continuously cooling for about 1,4 * 10^{21} J a year. (Lowrie 2007: 221, 228.)

Geoenergy on the other hand also includes solar energy that has warmed the upper layers of the earth. This is called ground source heat. It is usable in non-volcanic regions. The use of heat pumps allows this sort of geoenergy to be used in the heating of buildings. Other types of stored solar heat include asphalt heat, seabed sediment heat, watercourse heat and bedrock heat. The last one is most relevant to this study.

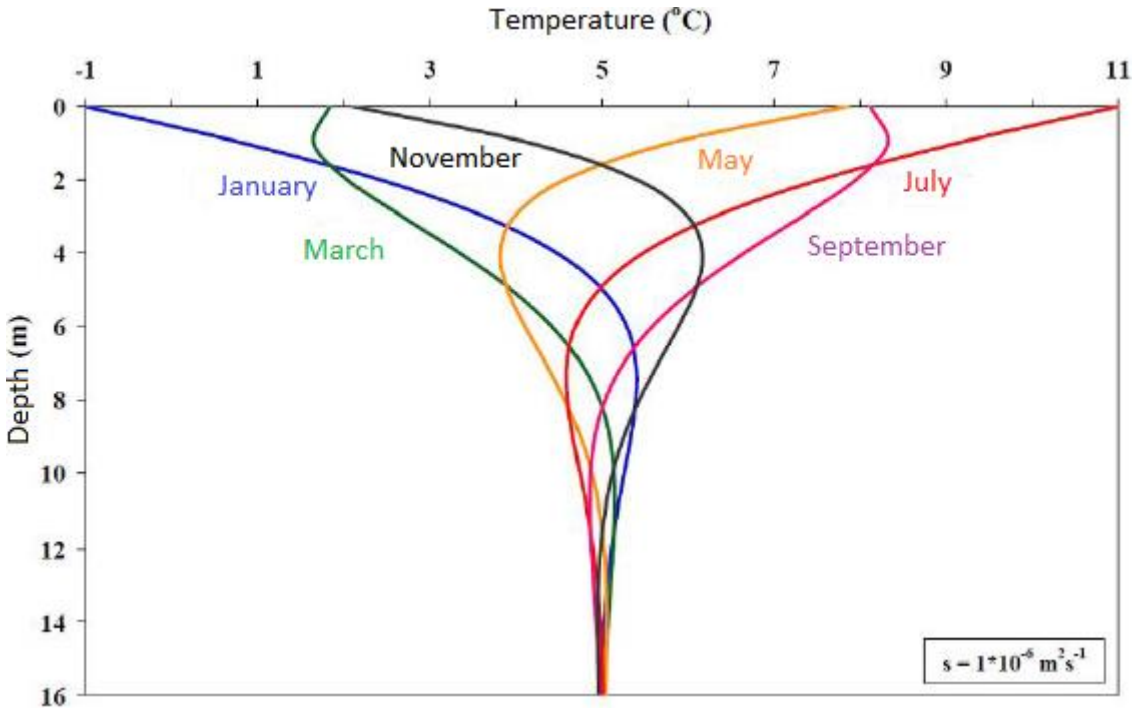

Figure 1. Ground temperature with depth and time of year. (Leppäharju 2008: 7).

The effect of yearly air temperature oscillations on bedrock temperature reaches 10 to 15 meters of depth in Finland. Daily variance reaches about half a meter deep. The earth's heat conductivity is small, its heat capacity large and there is plenty of rock mass. Therefore, at the aforementioned 10—15 m depth, temperature tends to be close to the above ground yearly average (Figure 1). From this can be deduced that solar heat is transferred some 1,25 m/month downwards on average. This physical phenomenon can technically be utilized for heating during cold periods and cooling in summertime.

Geothermal gradient – or the increase of temperature with depth is affected not only by the aforementioned factors such as decaying isotopes, but also by long-term surface temperature variations such as ice ages. The geothermal gradient is about 8—15 K/km, or one Celsius degree per hundred meters (Figure 2). (Leppäharju 2008: 6—9)

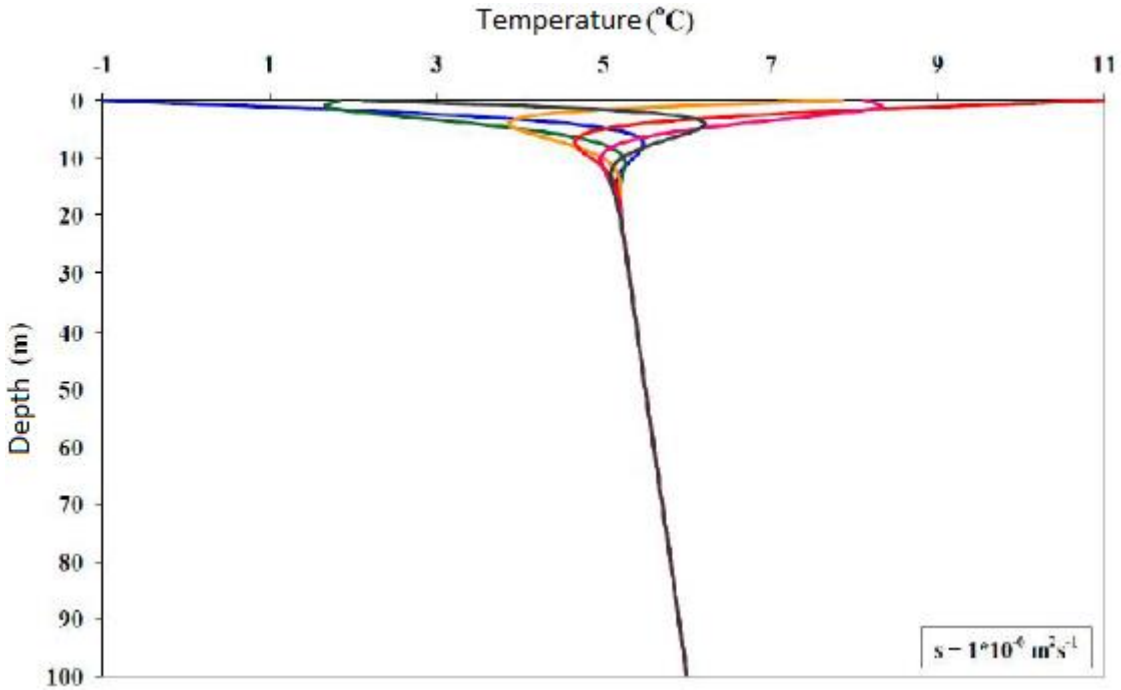

Figure 2. The geothermal gradient down to 100 meters. (Leppäharju 2008: 9)

Geological and hydrological factors affect the storing of heat to upper layers of the earth. Ground source heat's usability depends on the quality of soil and uniformity of

the rock. Especially groundwater and its flow should be taken into account when designing borehole heating systems. Finland's bedrock is mostly gneiss and granite without any volcanic activity. Heat collector pipes can be installed horizontally on shallow ground, but that requires too wide an area for many situations. Vertical boreholes have become more common.

Underwater sediment tends to contain more heat than the water. It is currently under research, where such heat originates. Supposedly, the majority of it is from the sunrays penetrating the water. The pipes are installed in a method similar to road under passing. After the drilling, pipes are attached to the drill and drawn backwards.

Out of a water system, heat can be extracted, because temperature near the bottom is usually some degrees above 0 °C. The technique used is the same with ground source heat. Pipes are sunk to the bottom of the sea with added weights.

Ground source heat is used by planting heat collector pipes in the ground under frost depth. During warm times of the year, heat from the sun is stored in upper layers of the ground. Some of it is transferred deeper. Cooling appliances can also be connected to a ground heating system. This way the ground can be "recharged" to some extent with surplus heat to be used for heating purposes later.

A BHE is implemented by drilling a deep hole into the bedrock. Heat collector pipes are led into the hole with weights attached. Required depth and number of holes depend on the heating requirements. Temperature of the ground gets warmer with increased depth. Costs of drilling also increase with depth. In Finland, boreholes for heating purposes are usually 100—200 meters deep. If 200 m is too shallow for heating requirements, more than one borehole is drilled. Distance between boreholes should be 10 m minimum (Aittomäki 2001: 18). Temperature at 200 m is 6 °C on average (Figure 2). (Syrjälä 2013: 10—12.)

Figure 3 illustrates the annual average air temperatures in Finland. Leppäharju (2008) calculates that due to snow coverage ground surface temperature is about 2 °C higher

than air on average. In addition, ground surface does not drop much below 0 °C even at winter, because phase change from water to ice relieves some heat. Frost depth in Finland tends to be between 0,5—2 m depending on latitude (Rantamäki, Jääskeläinen & Tammirinne 2006: 120—122).

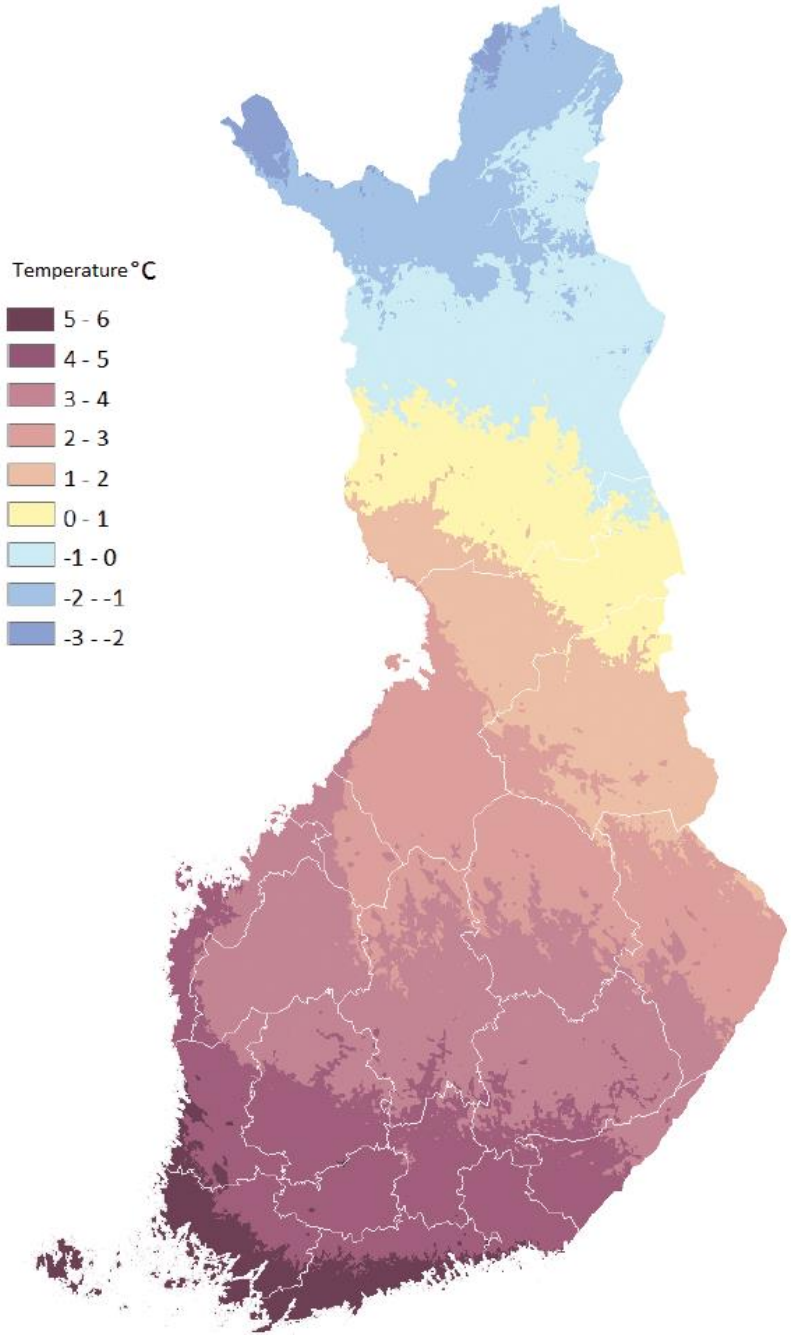

Figure 3. Mean year-round air temperature. (Pirinen, Simola, Aalto, Kaukoranta, Karlsson & Ruuhela 2012: 82)

2.1. Heat pump technology

Heat is collected from a ground loop via carrier fluid – usually a water-ethanol mixture due to its low freezing point. The carrier fluid is circulated with a pump. The heat is

transferred from the carrier fluid to a refrigerant in an evaporator. An electrically powered compressor is used to heat up the refrigerant, which is then led to a condenser, where it transfers the heat to a heat distribution system. (Figure 4) The amount of electrical energy required to operate a heat pump is supposed to be smaller than the heat energy produced. The ratio between these is called the coefficient of performance (COP), which is usually around 3 in Finland. (Aittomäki 2001.)

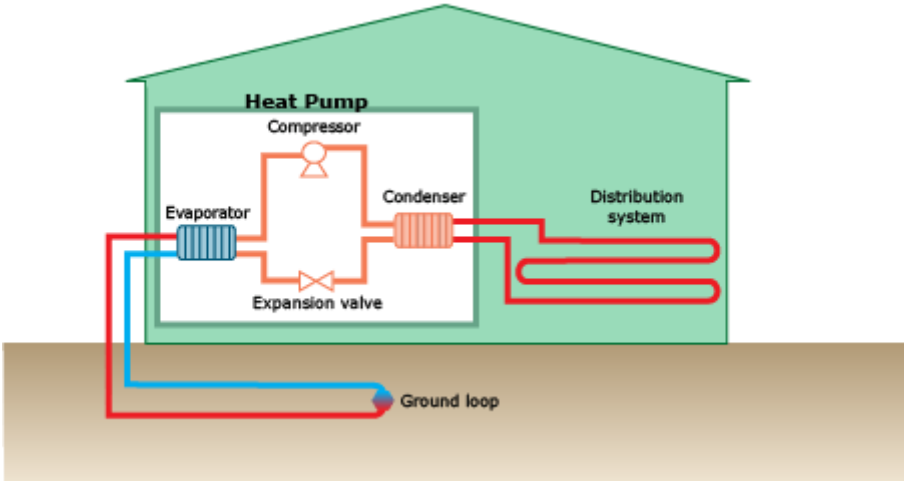

Figure 4. Heat pump operation. (BASIX 2016)

A high evaporation and a low condensing temperature are ideal for a good COP. In other words, this means a minimal compressor output. A high heat source temperature allows a higher evaporation point. The condensing temperature is determined by the heat distribution system. Water circulation based floor heating usually accomplishes the lowest, down to 30 °C condensing temperature. Air heating can also have low requirements. (Aittomäki, 2001; Seppänen, 2001.)

In BHEs, pipes of polyethylene or their derivatives are commonly used. In addition to conventional U-pipes (Figure 5), coaxial pipes have been developed (Figure 6). Those have a central pipe and a number of side channels to improve heat transfer with the surroundings. The heat carrier fluid circulates downwards through the side channels and upwards through the central pipe. This is to reduce thermal short-circuiting (cf. Acuña

& Palm 2010: 5). There are also metallic spiral pipes. Those have greater thermal conductivity due to form and material.

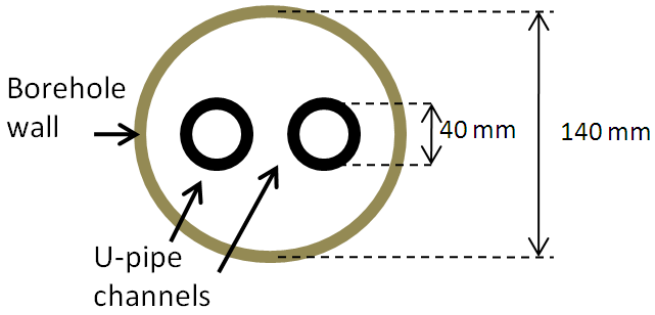

Figure 5. U-pipe. (Acuña & Palm, 2010)

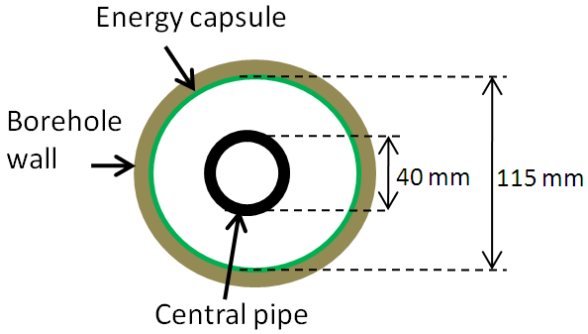

Figure 6. Coaxial pipe. (Acunã & Palm, 2010)

It seems 55 % of new buildings in Finland choose ground or bedrock heat as their heating solution (Rakennustutkimus RTS Oy, 2016). In the year 2014, 64 TWh of energy was used by housing in Finland. 56 TWh or 63 % of that was used for interior and water heating. Household appliances used the rest. Ground-source heat pumps are approximated as having extracted 2,2 TWh of heat from the environment and air heat pumps 2,4 TWh respectively (Figure 7). (Official Statistics of Finland 2015.)

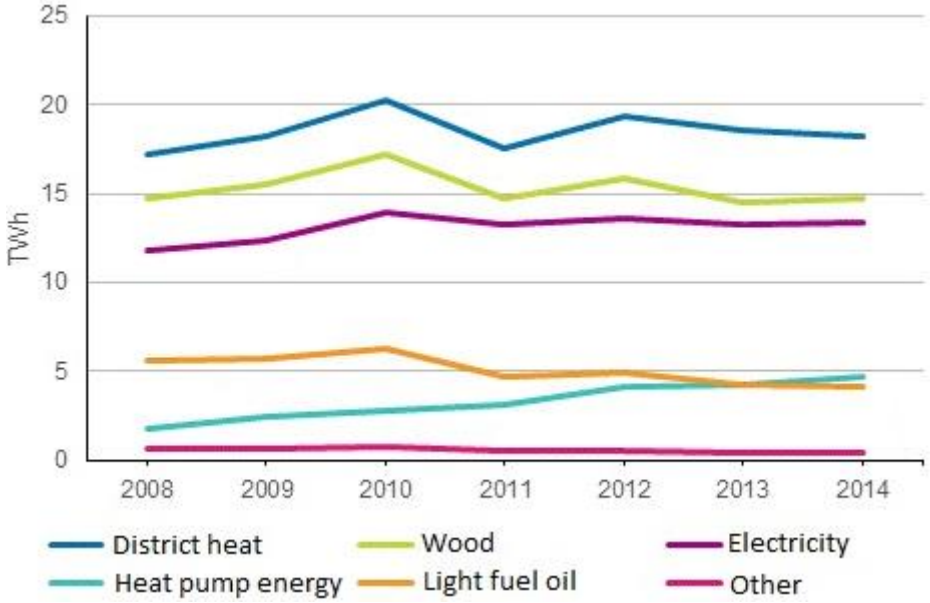

Figure 7. Heating of residential buildings in Finland. Turquoise line indicates combined ground and air source heat pump energy. (Official Statistics of Finland 2015)

After 25 years of heat extraction 32 % of heat flowing to a BHE originates from above ground. The rest are from the rock surrounding the BHE. After a hundred years, half of it is from above ground. After a thousand years, only 15 % is calculated to be still from the cooling of the surrounding earth. In addition, one third of the surrounding earth's cooling happens on the first day of heat extraction. After a month, two thirds are depleted. After 5 years, the surrounding rock's temperature does not change much. (Claesson & Eskilson 1987: 9, 12.)

2.2. Underground thermal energy storage

Underground thermal energy storage (UTES) means to store energy in the form of heat underground. There are multiple ways to do this. These include cavern, water tank, aquifer and borehole storage solutions. The last two are relevant to this thesis. UTES technology has a high maturity level compared to most other forms of energy storage (IEA 2014: 16).

One reason to store heat underground is that thermal energy is technically cheaper to store than electricity. Another reason is that there may be heating needs in the winter and cooling needs in the summer. Injecting and extracting heat from the store is an economical way to meet these needs. Circulating a fluid as a heat carrier with the aid of a heat pump is one way to apply heat transfer physics in accomplishing this. In addition, energy price fluctuations on the Nord Pool market could possibly be stabilized to some extent with energy storage (Harris 2011: 11–12). Said fluctuations are chiefly caused by intermittent renewable energy generation such as wind power.

Twenty years ago, researchers from the Technical University of Munich attested that seasonal thermal energy storage (STES) technology should be made fully operational as soon as possible. This is to increase efficiency of conventional energy sources. Additionally, substituting them with renewables such as solar requires some form of storage. Apparently, duct systems with vertical heat exchangers could very well be built onto areas with no groundwater or low flow velocities. Technically and economically, it would be most feasible to store heat seasonally in the ground with temperature ranging up to 90 °C. They used an underground duct system to store industrial heat. They managed to reuse 266 MWh/a of the stored 418 MWh/a thermal energy that would have otherwise been lost. The price for this energy was calculated to be close to other energy sources such as liquid gas. (Reuss, Beck & Müller 1997.)

Stratification of energy stores allows heat to more easily be added to colder parts of the store. Meanwhile, hotter parts have higher quality energy for extraction. The Drake Landing Solar Community used this principle with an array of vertical boreholes (Figure 8) while the Vaulruz system did the same with horizontal tubes superposed vertically. (Pinel, Cruickshank, Beausoleil-Morrison & Wills 2011: 3350—3351.)

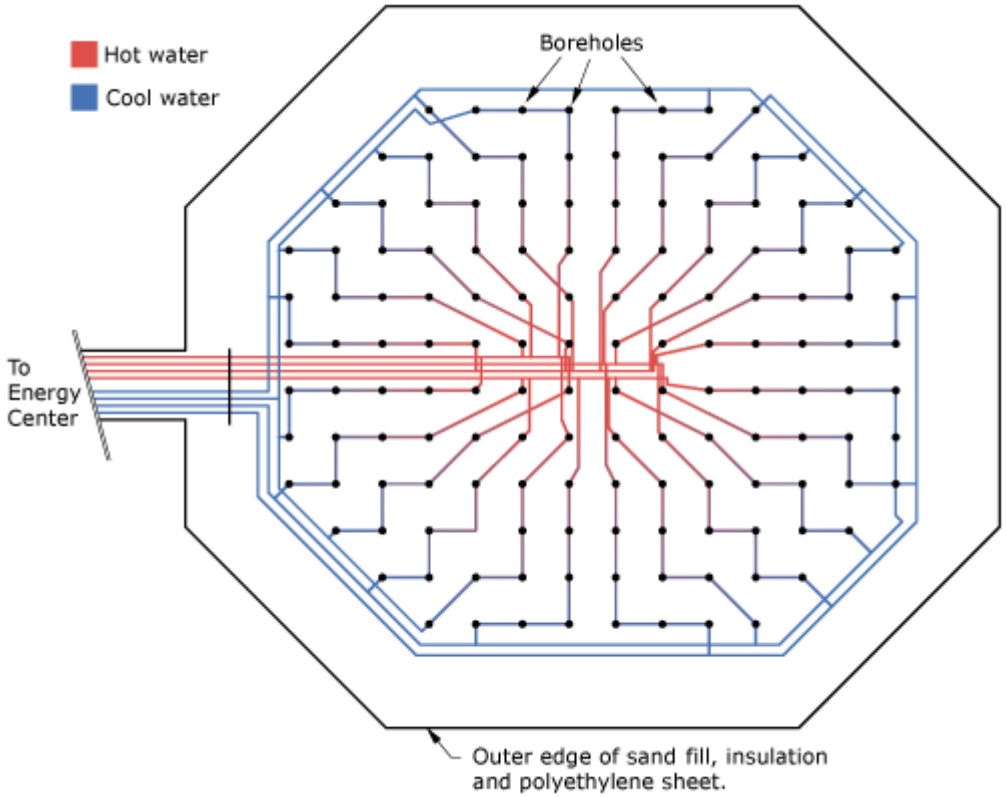

Figure 8. BTES array of the Drake Landing Solar Community. (DLSC 2017)

In Sweden, there are already many instances of TES. One was built at Luleå University of Technology as early as 1982. It had 120 boreholes 60 m of depth. It was heated by waste heat from a local steel plant. The heat was pumped to the store using the district heating infrastructure. The store was in operation from 1983 to 1989 and retained 1000-1200 MWh of its injected 2000 MWh heat. (Nordell 1994; Hellström 2012.)

Another example is the Emmaboda BTES, which has been operational from the year 2010 onward. Its 141 holes are 148,5 m deep. From its 3600 kWh of injected waste heat in the summer, 2000 kWh could be extracted in the winter for space heating. Furthermore, the Arlanda Airport has an aquifer thermal energy storage (ATES) system. It paid its investment costs back in 6—7 years with 3—4 GWh of electricity and 10—15 GWh of heat savings. Drilling costs in Sweden are approximated as 20-35 euro/m. Other costs total 1500 euro per kW of heating capacity, which includes the heat pump, heat exchanger and their installation. (Hellström 2012.)

2.3. Geoenergy research in the University of Vaasa

Near the University of Vaasa, a comprehensive system of geoenergy use is being built: Underwater sediment heat (picture 2), asphalt heat (picture 1), ground source heat and water system heat.

Picture 1. Parking lot with vertical optical fiber cables underneath.

Under a parking lot, there are vertical optical fiber cables down to 10 meters. Over several years, measurements are being made at least once per month. A future possibility is to construct an asphalt heat-utilizing field somewhere nearby. Now measurements are being used to determine how heat reacts in the different layers of the ground. In addition, the usability of asphalt heat in a way similar to ground source heat is being considered.

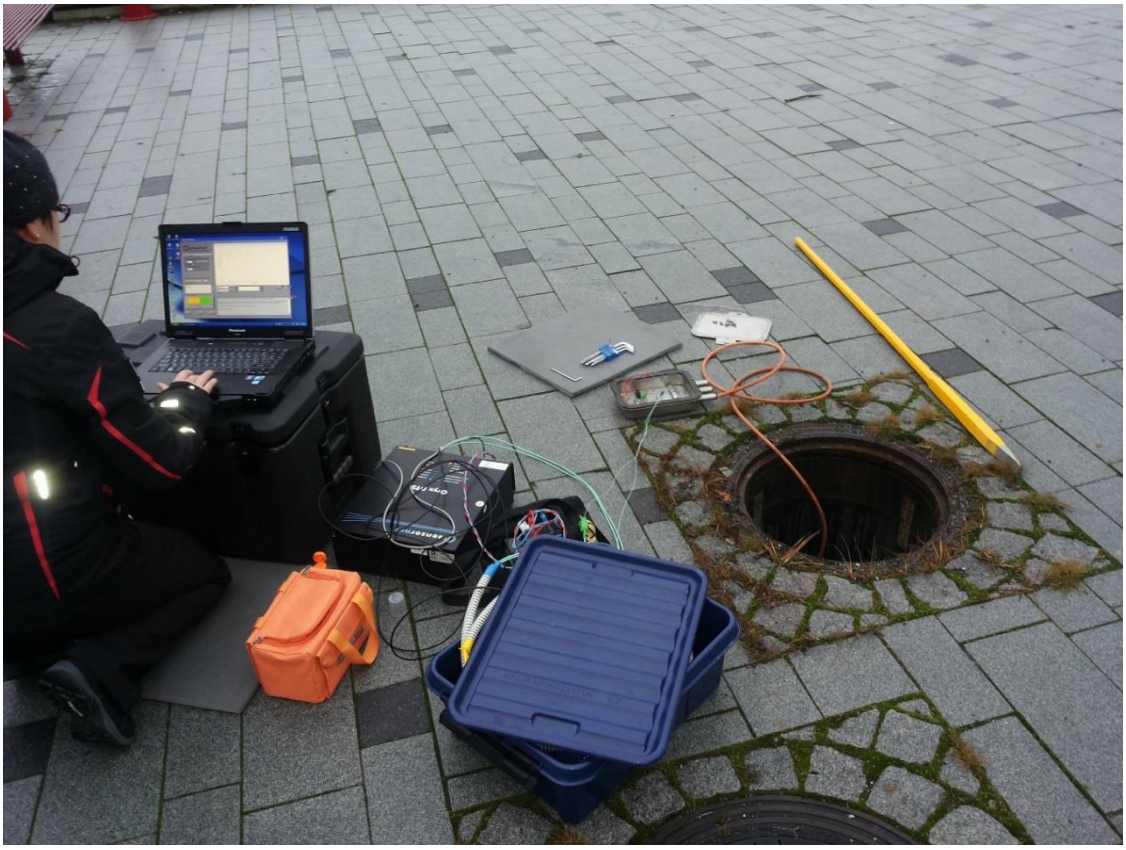

Picture 2. Well in Ketunkatu.

At the Suvilahti housing fair area, 26 coaxial heat collectors have been dug horizontally 3—4 m deep into the seabed sediment (Figure 9). The pipes are 300 m of length. Two of the pipes have an optical fiber attached – one starting from Ketunkatu and another from Liito-Oravankatu (Figure 10). Their temperatures are measured at least once a month using DTS technology. Currently, the pipes are being used to heat and cool buildings in the area depending on the time of year.

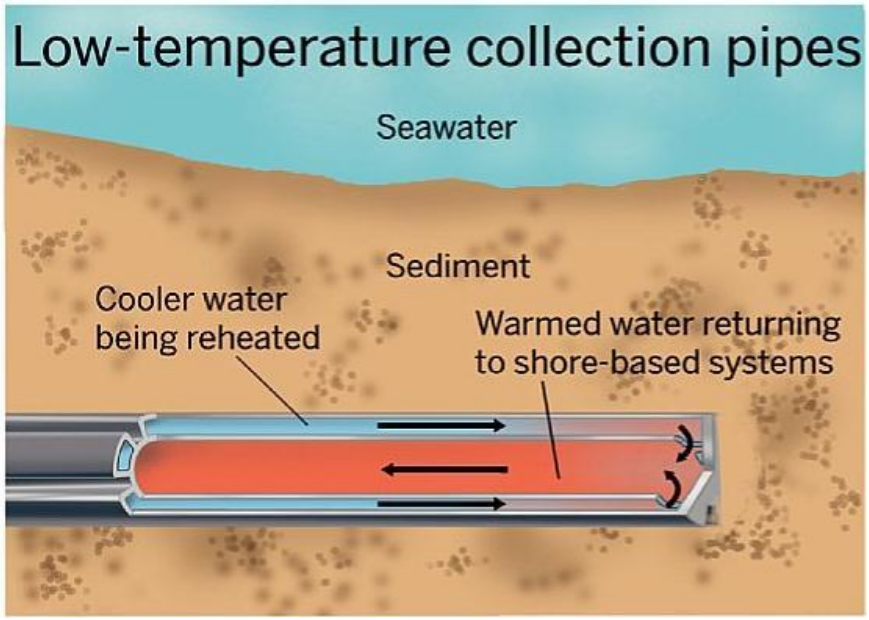

Figure 9. Sediment heat collection pipe **(**Mauri Lieskoski 2013).

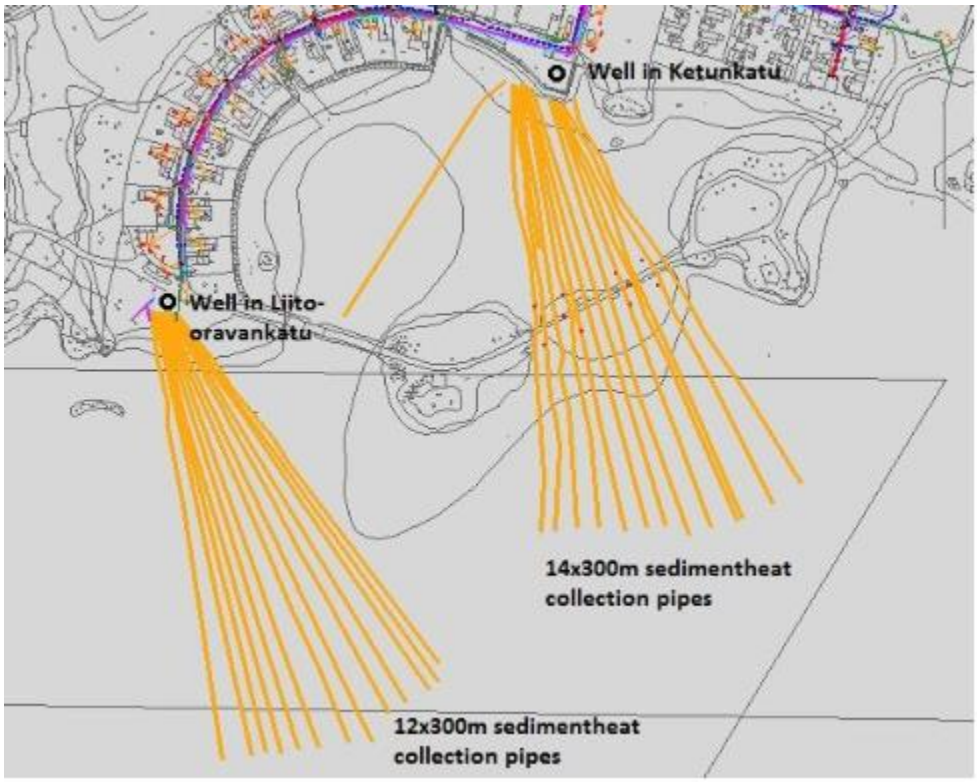

Figure 10. Suvilahti sediment heat (Vaasan vesi 2013).

3. THERMAL RESPONSE TEST

3.1. TRT-measurements

A TRT is used to find out thermal properties of the ground. Specifically there are two important properties, thermal conductivity of the ground and thermal resistance between the ground and the installed heat exchanger. These are of interest to designers of ground source heating systems. Such parameters are used to calculate the required number, spacing and depth of holes to be drilled to fulfill heating requirements. Kavanaugh (2000) predicted that from a 10 % divergence in thermal conductivity followed a 4,5—5,8 % error in design length for a 351 kW office building. Such a small error had no noticeable effect on COP. Figure 11 lays bare a TRT unit.

Lord Kelvin is credited for laying a foundation for what was to become the thermal response test. Mogensen first suggested a test configuration that had a U-tube, a cooling machine and a sensor for temperature logging in the year 1983. In Sweden and the United States mobile test rigs were developed independently around the mid-1990. Commercial tests utilizing best available technology today are not considerably different from the ones performed in 1996. There have been numerous improvements, such as new mathematical methods for result interpretation, better error analyses and adjusting for changing air temperature. In addition, many aspects of the complicated issue of groundwater have been discussed. (Spitler & Gehlin 2015: 1134—1135.)

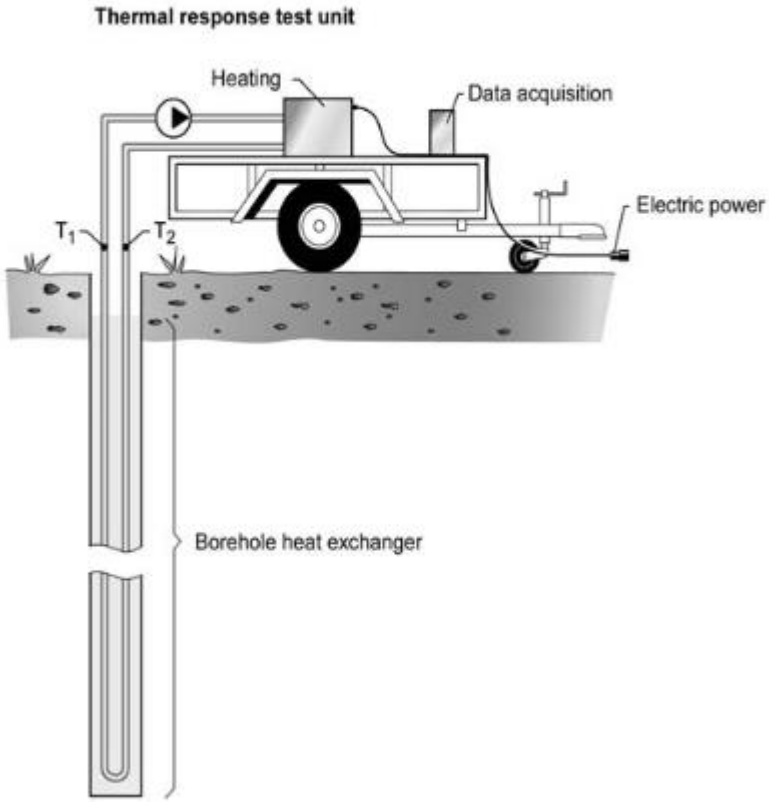

Figure 11. Thermal response test unit (Gehlin 2002).

3.2. TRT and groundwater

Groundwater flow adds a remarkable difficulty to interpreting TRT results. In some cases, it may even render test results useless (Sanner, Hellström, Spitler & Gehlin 2005: 4). Several authors have published papers dealing with the issue.

Witte did heating and cooling tests in 2001. It would seem like the heating test does not produce representative results in saturated ground conditions (Figure 12). 10 to 15% greater conductivity was measured apparently due to convection in and around the borehole. Also, significant losses are to be expected if the borehole heat exchanger (BHE) is to be used as a heat storage in an area with passing groundwater flow. Witte suggested directions for further research: 1. temperature logs at different depths 2. effects of convection 3. effects of groundwater flow, and how to incorporate that in the final design of a BHE system.

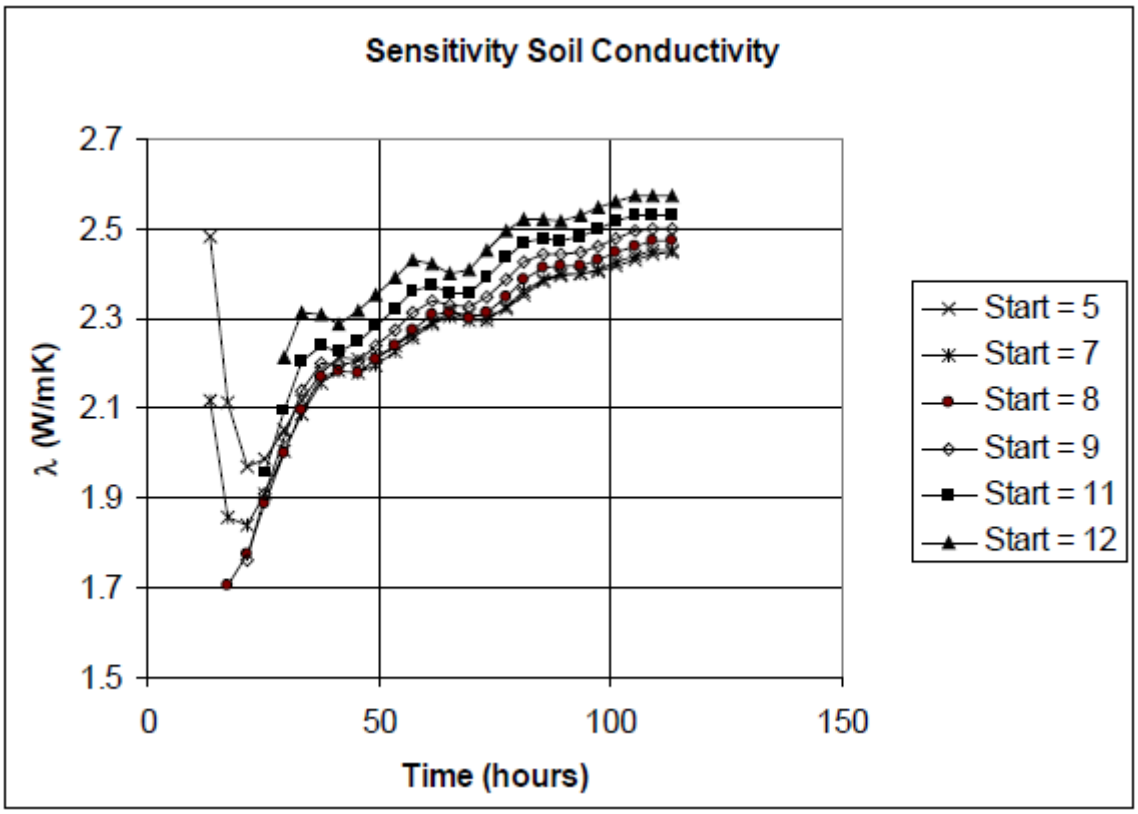

Figure 12. Measured thermal conductivity changing with time in saturated ground conditions. (Witte 2001)

Gehlin, Hellström & Nordell (2003) studied the thermosiphon effect induced by TRTs. Due to heat injection water goes through heat expansion. If in the bedrock there are fractures intersecting a BHE, heated water may exit the borehole through the upper parts. Ambient temperature water from a fracture closer to bottom will flow to replace that. This creates an upwards flow in the aquifer. This affects to the measurement result. They suggested that heat injection and extraction on the same borehole might provide information about the potential for thermosiphon effect. They also mention that a temperature profile along the borehole may provide information about this phenomenon.

Gustafsson (2006) also did a heating and cooling test. They had some equipment control problems resulting in some cooling power fluctuations. Because heating and cooling parts of the test produced nearly identical results, their test confirmed assumptions of minimal groundwater influence.

Signorelli, Bassetti, Pahud & Kohl (2007) did a numerical model taking into account groundwater. They attested that in an area with significant groundwater flow, results from a TRT should be paired with an analysis of groundwater effect when designing a BHE system. Wagner, Blum, Kübert & Bayer (2013) did an analytical calculus model that also includes groundwater effect. This was based on a moving line source theory.

Coleman, Parker, Maldaner & Mondanos (2015) did a DTS heat pulse test to acquire information about groundwater movement in a fractured bedrock environment. They pointed out that it is difficult to differentiate what portion of heat dissipation is caused by geologic factors or groundwater. They suggest that separate heating and cooling phases may provide additional information.

Scorpo, Nordell & Gehlin (2016) possibly found a way to differentiate groundwater advection from TRT results. Some imperfections in the method are yet to be overcome.

There is some controversy in the industry regarding the minimum test period of a TRT. Some Swedish authoritative people say 50 hours is the minimum measurement period of a TRT. This is also the official opinion of the IEA (2013). Shorter 12-hour duration would make it commercially more viable, without the need to have the test rig on site overnight. It would appear that a test period of 50 hours yields up to 5% error, and a 20-hour test might err up to 15%. (Sanner et al. 2005: 2.)

It would appear that based upon previous research and their authors' suggestions, the next logical step would be to perform a heat injection and extraction test where temperatures are measured along the full length of a borehole. Many have assumed that this would give some insight into the many nuances of groundwater effect on ground thermal properties.

4. DISTRIBUTED TEMPERATURE SENSING

A distributed thermal response test (DTRT) means a TRT featuring depth distribution of measured temperature data. Distributed temperature sensing (DTS) can measure temperature distributions over the length of an optical fiber. There appears to be applications with ranges up to 150 km. It uses optical fiber cable as a line-shaped sensor. Sampling resolution, or distance increments between the temperatures measured, depends on the settings, but is usually 1 m. Figure 13 shows an example graph of measurement results. According to LIOS Technology (2015), the measuring device consists of a frequency generator, laser source, optical module, high frequency mixer, receiver and microprocessor unit.

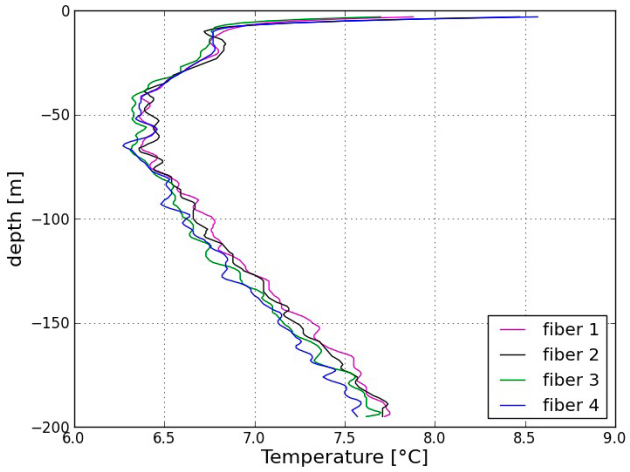

Figure 13. Undisturbed ground temperature graph. (GTK 2014)

The device sends a short, 10 nanosecond or less (Smolen & van der Spek, 2003: 8), light pulse to the fiber. Some of the light scatters back towards the receiver. Temperature can be calculated from the relative signal strength between light of different wavelengths that return to the device. Since the speed of light is a constant, distance can be calculated from the light particles' back and forth time travelled, similar to radar. Accuracy of the device being used is ±0,5 °C (Mäkiranta 2013: 30).

The DTRT procedure and interpretation of the results takes about three times longer than a conventional TRT (Hakala, A. Martinkauppi, I. Martinkauppi, Leppäharju & Korhonen 2014: 7). Even water flow inside a structure can be measured provided that the flow produces heat differences (Englund, Mitrunen, Lehtiniemi & Ipatti 2008: 26). The fiber is economical compared to having many sensors, but the controller unit is expensive.

When a light pulse from the DTS device interacts with molecules of the glass fiber, certain phenomena happen that cannot be properly understood without knowledge of quantum physics. For engineering purposes, it is sufficient to know that some of the light scatters when it collides with matter. Quimby (2006: 57) states that light can pass an ideal crystal at zero Kelvins without scattering. A material that has impurities, or simply does not have a crystalline structure, is going to cause light to scatter. Air and glass are examples of such materials. According to Powers (1997: 37), "scattering losses occur when a wave interacts with a particle in a way that removes energy in the directional propagating wave and transfers it to other directions."

Tiny fractions of the scattered light have its wavelength increased and others have it decreased in a symmetrical manner. This is partially due to heat-induced vibration of electrons. With an accurate enough device, temperature-dependent part of the backscattered photons of light can be measured with sublime precision. Quimby (2006: 61) said the following about light scattering's temperature dependency: "At finite temperature, there is some probability that the molecule is initially in the ground vibrational state, in which case no energy can be extracted. Therefore, the ratio of anti-Stokes to Stokes scattering probabilities is less than one, and is temperature dependent." Temperature measuring is based on this physical phenomenon.

Most of the scattered light is elastic Rayleigh scattering, which does not have its wavelength altered (Figure 14). This is used in calibrating the device. Some photons receive energy from the vibrating electrons they pass through resulting in higher frequency. Similar to a Doppler effect, other photons lose energy due to the same vibration. These are called anti-Stokes and Stokes photons respectively. The exchange

of energy happens by something called a virtual state - the understanding of which is not required here.

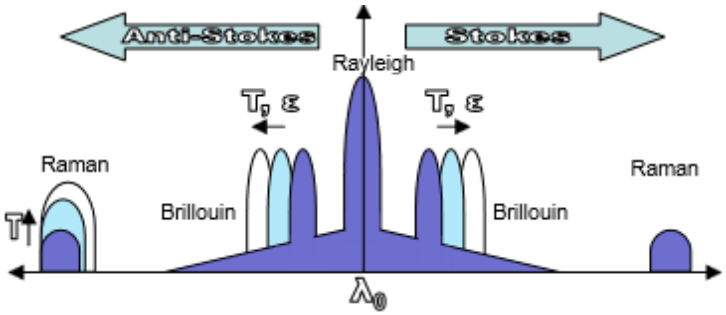

Figure 14. Stokes and anti-Stokes scattering. (Englund et al. 2008: 6)

Raman scattering occurs when light hits a vibrating molecule. The other two types (Figure 14) have to do with nonhomogenic spots in the fiber due to manufacturing. Raman and Brillouin scatterings appear on both sides of the wavelength, as seen in the above figure. Such light particles of longer and shorter wavelength are called Stokes- and anti-Stokes components respectively. Anti-Stokes Raman scattering is sensitive to temperature. The Stokes one is not. In the formula used to calculate temperature, a comparison between the two is used (Formula 1). Brillouin scattering is dependent on both temperature and strain of the fiber. Strain measurements are not needed in a DTRT.

$$T(z) = T_{ref}\left(1 + \frac{\Delta\alpha z}{\ln\frac{C_+}{C_-}} + \frac{\ln\frac{I_+(z)}{I_-(z)}}{\ln\frac{C_+}{C_-}}\right) \quad (1)$$

T, temperature, K.

z, distance, m.

Δα, attenuation, 1/m.

C_+ and C_- are constants.

$I_+(z)$, Stokes band energy, dB/m.

$I_-(z)$, anti-Stokes band energy, dB/m.

Equation 1 (Smolen & van der Spek 2003: 80) is a simplification. The first term represents the offset and the third term is the temperature measured. The second term is the differential attenuation that takes into account signal decay over distance.

An optical fiber cable has fibers for measurement and data transfer. The cables are made of doped quartz glass. They can be even kilometers long. There are single- and multimode types of fibers, which have some differing properties. Stokes and anti-Stokes signals decay marginally over distance. The attenuation coefficient attempts to compensate for this in the formula. Splices and breakages cause step loss points in the data. The cable itself has a coating and a cladding around the core (Figure 15, Picture 3). The measuring equipment must be calibrated before use. This is done by placing the fiber through 0 °C ice water.

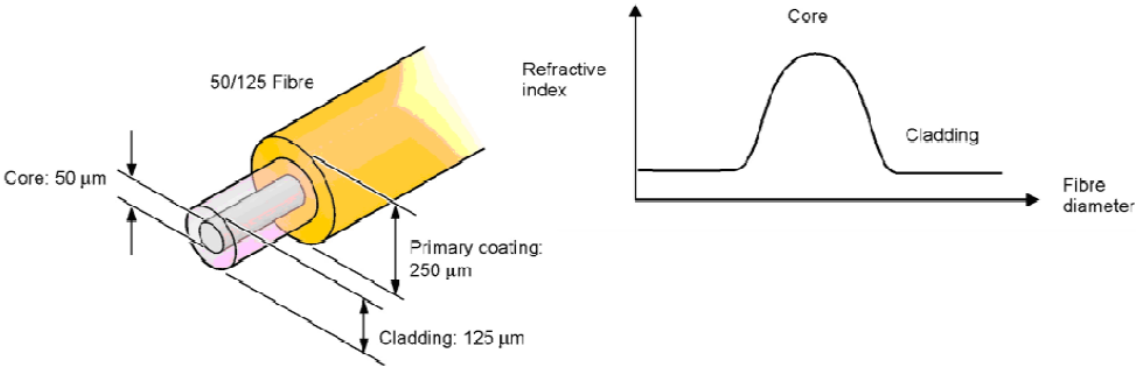

Figure 15. Structure of a fiber cable. (Sensornet 2007)

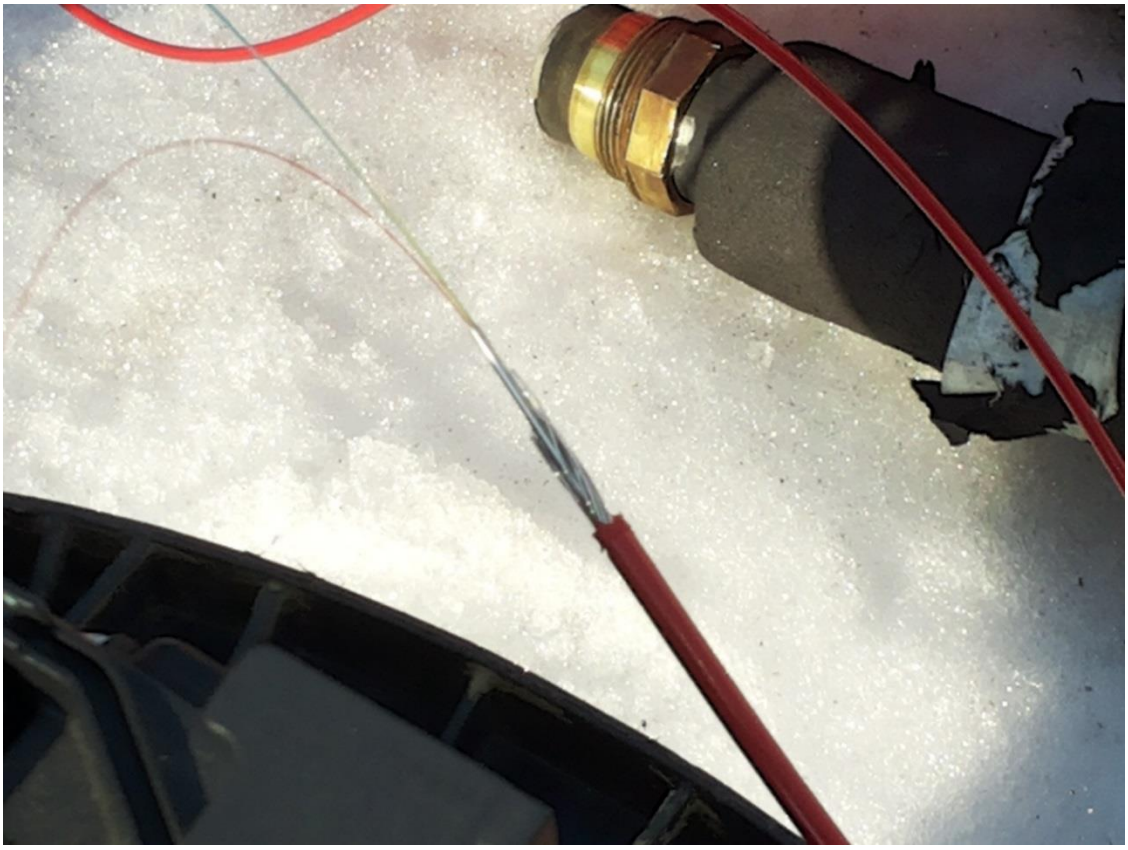

Picture 3. Optical fiber used for measurement.

Several authors have published papers where DTS is used to measure temperature profiles along a BHE. For example, Acuña & Palm (2010) used it to test a new pipe design. Hakala et al. (2014) in a study of Geological Survey of Finland evaluated the method with a case study, in which they did measurements with a heating and recovery period. They did not take the effect of groundwater into account when interpreting the results. Hakala et al. found that ambient temperature variations due to day/night cycles may affect the results up to 2 °C.

5. METHODOLOGY

From here on is the empirical part of this thesis. The research BHE is 122 m deep. It is located in Gerby, Vaasa. Groundwater saturated zone starts 1,39 m below the surface of the ground. It is estimated that in this case about 85 % of heat originates from the sun as opposed to other, more geothermic sources. The BHE has a conventional U-pipe installed. Soil type is sandy moraine according to the National Land Survey of Finland (2013). Rock type is granodiorite, commonly called Vaasa's granite. Time of year is the middle of spring. There was still some snow around (picture 4).

Picture 4. TRT-trailer on site.

At first, the heat carrier fluid was circulated overnight without heating between Wednesday and Thursday. The fluid is a 30 % ethanol-water mixture. Its freezing point is about -20 °C (Melinder 2007: 8). On Thursday a 6 kW resistor was activated. The rest of the experiment a 7,1 kW heat pump was used during the day. Resistor heating did not

require research personnel to be present unlike the heat pump and condenser usage. Therefore heating was done during nights and cooling during days between 9:00—16:00. The test was carried on for four days between 11.4 and 14.4.2016. At 15.4 morning, the BHE was allowed to recover for some hours. Some modifications to the test unit are being implemented to allow for longer cooling periods in future tests without the need for live supervision. The test equipment are being developed to remove the need for a human to be present. This allows for longer cooling periods by heat pump.

The volumetric flow rate of the heat carrier fluid was about 0,59 dm^3/s during heating and 0,52 dm^3/s with cooling. The difference follows from a change in viscosity with temperature. Pressure in the pipe leading to the BHE was around 179 kPa. The flow rate was chosen as such to cause turbulent flow (Syrjälä 2013: 21).

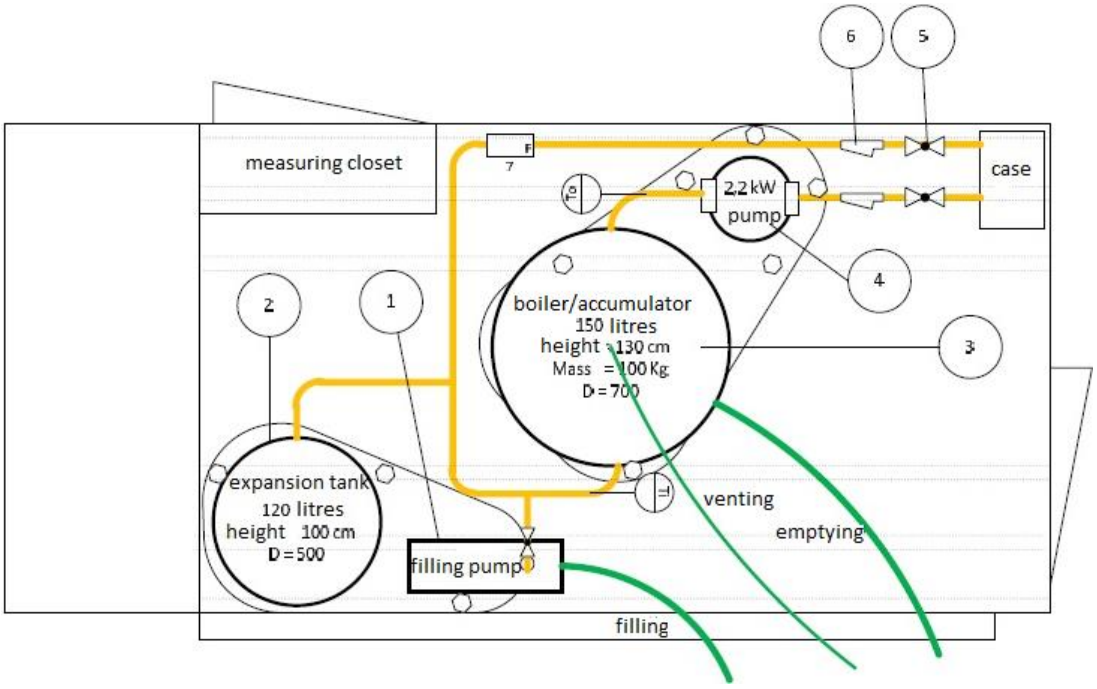

Figure 16. Original sketch for the layout of the TRT-trailer. (Syrjälä 2013: 72)

Figure 16 and picture 5 exhibit the test unit's equipment and layout. Figure 16 is not entirely accurate as the measuring closet is actually in the front of the trailer and a heat

pump is situated in its place. In addition, there is a condensing fan in the rear. There was also the DTS device, which is not in picture 5.

Picture 5. Insides of the TRT-trailer.

Pt-100 sensors for temperature measuring were present, but they were not submerged in the liquid due to some physical limitations imposed by the heat pump. Thus, the measurements were carried out mainly with DTS. A double-ended measurement setup was used. There were four times 122 m fiber cables in the U-pipe – two inside the entrance with a fusion splice joint at the bottom (Picture 6), and the same with the pipe's exit. The fusion splice causes only a 0,01—0,03 dB signal loss (Tyler, Selker, Hausner, Hatch, Torgersen, Thodal & Schladow 2009: 8). Measurements were programmed to be carried out every 10 minutes with a 1 m sampling resolution.

Picture 6. The making of fusion splice. Bottom right is the splicing device.

A water-ethanol mixture was circulated in a U-pipe with a pump. The fluid was first heated and then in turn bi-directional heated and cooled for four days. Along the length of the pipe, temperature was measured periodically with a laser beam. The measurement method is based on the Raman effect in light scattering. Results of the temperature measurement indicate possible groundwater movements through the BHE.

The fiber used was one designed specifically for measurement purposes. It was thin with a low heat capacity coating, with good responsivity to temperature changes.

The DTS device was calibrated using a bath of ice water. This calibration box was confirmed to be -0,14 °C with a few different thermometers (Picture 7). This is used in determining the offset coefficient needed in calculations of temperature. The ice water bath minimizes measurement error if the offsets value were to change for any reason,

such as ambient temperature changes near the DTS-device during a long measurement period (Tyler et al. 2009: 9—10).

Picture 7. Calibration box with triple checked 0 °C including both digital and analog thermometers.

The BHE is water-filled. Depth of the ground layer is unknown, but it appears Rototec Oy have drilled multiple BHEs in the Vaasa region. The ground layer atop bedrock has varied between 2—12 m in these locations (Rototec 2016). According to IEA (2013: 17), ground layers thinner than 10 m need not be taken into account in TRT-related calculations, even though ground tends to have a lower conductivity than rock.

Heating-induced convection, horizontal or vertical, may affect results at least in the heating phase. Sanner et al. (2005: 4) state that vertical convection occurs only at open

boreholes, poorly grouted holes or ones grouted with sand. The research BHE was closed and filled with water.

The tubes above ground, including parts inside the trailer, were insulated with 19 mm thick Armaflex cell rubber foam to prevent diurnal temperature variations from affecting results (Picture 8). The trailer had a weather tower, which was used to log outdoor temperature along with other weather variables, such as wind strength and direction (picture 9).

Picture 8. Pipe insulation featuring optical fibers.

Picture 9. Weather tower and measuring closet.

Effective cooling power was calculated as follows:

$$P_{cooling} = C_p \times \dot{V} \times \rho \times (T_{out} - T_{in}) \quad (2)$$

P, cooling power, W.

C_p, specific heat, J/(kg*K).

$\dot{V}$, volumetric flow rate, m^3/s.

ρ, density, kg/m^3

T, temperature, K.

Picture 10. Settings panel of the TRT-trailer featuring a computer and a frequency converter.

Interpreted from Melinder's (2007: 12, 15) graphs the density of 30 mass-% ethyl alcohol is 950 kg/m^3 and specific heat is 4300 J/(kg*K). Between temperatures of -5 °C and 20 °C, the changes in ethyl alcohol's specific heat and density are negligible – not much more than one percent. Volumetric flow rate during all of the cooling phases was a reasonably steady 0,52 dm^3/s.

The Pt-100 sensors could not be submerged in the liquid during the cooling phase due to physical limitations. Having them attached to the exterior of the pipe did not produce usable results either (Figure 16). Because of this, the difference between inlet and outlet

temperatures was calculated more indirectly using DTS. The mean between the 10 first meters below ground was chosen as the inlet temperature. The first meter nearest to surface was excluded because weather affected it too much. The same was done with the exit pipe. The difference between these approximated inlet and outlet temperatures is shown on the graph below as a point (Figure 17). As can be seen, the difference varies with time. Furthermore, the mean between these, 3,36 K, was used in calculating effective cooling power. The first and second points on the graph were ignored.

Picture 10 shows cooling power to be 8 kW. With formula 2

$$4300\ {}^{J}/_{kgK} \times 0{,}52\ {}^{dm^3}/_{s} \times 0{,}95\ {}^{kg}/_{dm^3} \times 3{,}36\ K = 7{,}1\ kW, \qquad (3)$$

calculated cooling power was found to be smaller.

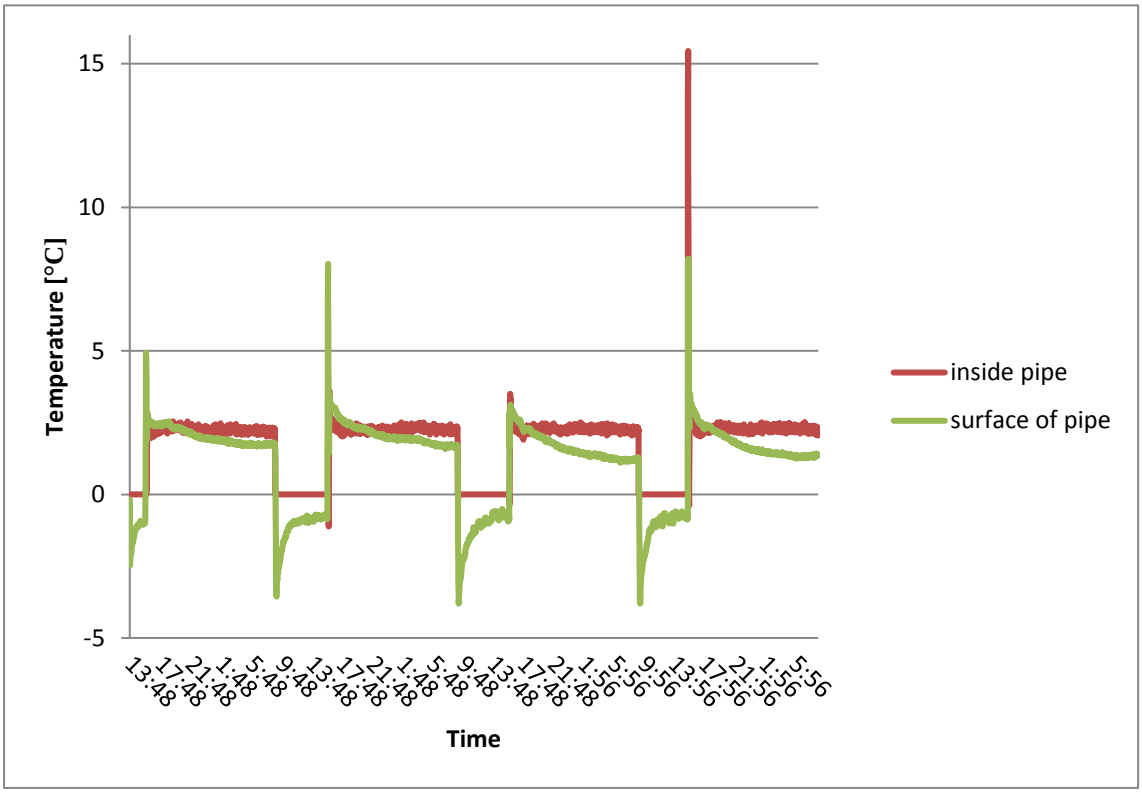

Figure 16. Pt-100 sensor output during heating and cooling phases. The subtraction of inlet-outlet temperatures ($T_{avg} = T_{in} - T_{out}$). The results from sensors attached to the outside surface of the pipe were not found usable.

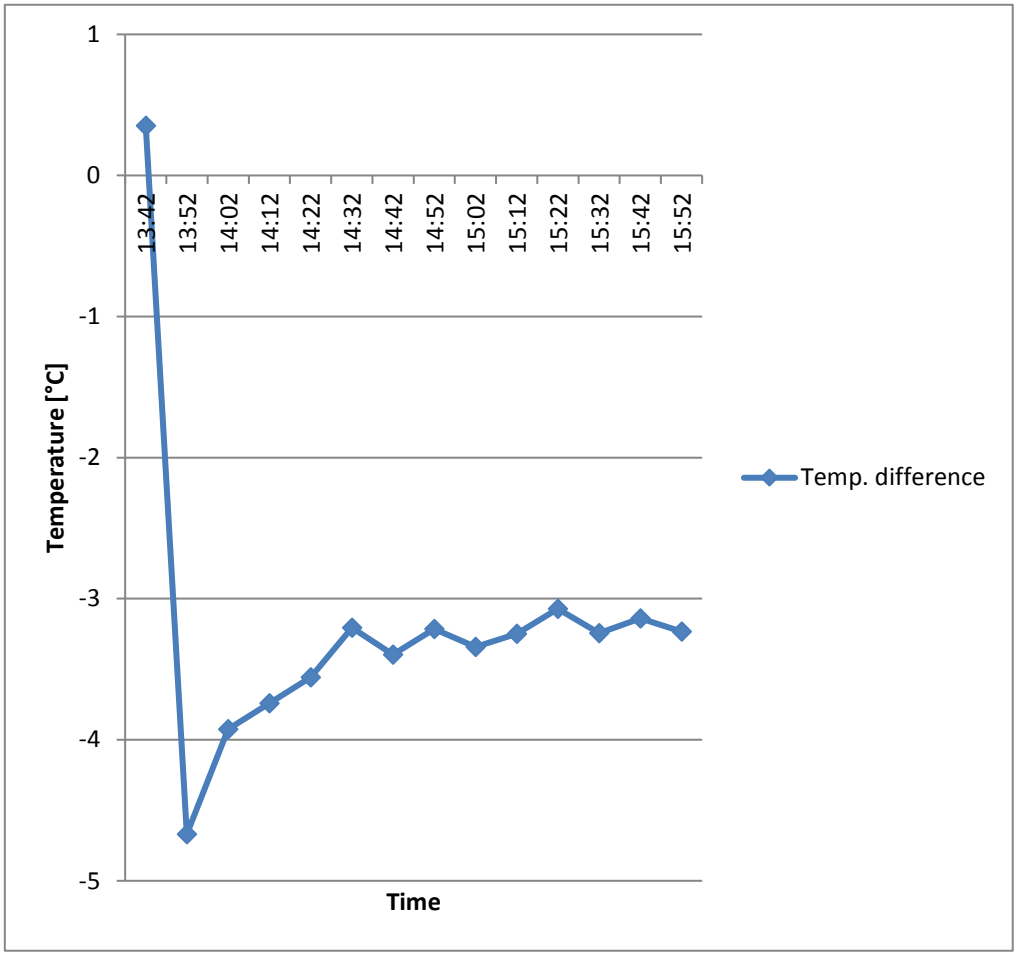

Figure 17. Temperature difference between inlet and outlet during the first cooling phase. This was used in calculating effective cooling power.

6. RESULTS

6.1. Undisturbed ground temperature

Ambient ground temperature before heating was measured mostly because it is needed in calculus formulae. There are many ways to determine it. One of them is circulating the heat carrier fluid while measuring its temperature.

The initial ground temperature was determined with Figure 18. It has been suggested (Zhang, Guo, Liu, Cong & Peng 2014: 854) that only the first 30 minutes of circulation without heating should be taken into account. In this case that would be 5,4 °C (Figure 18).

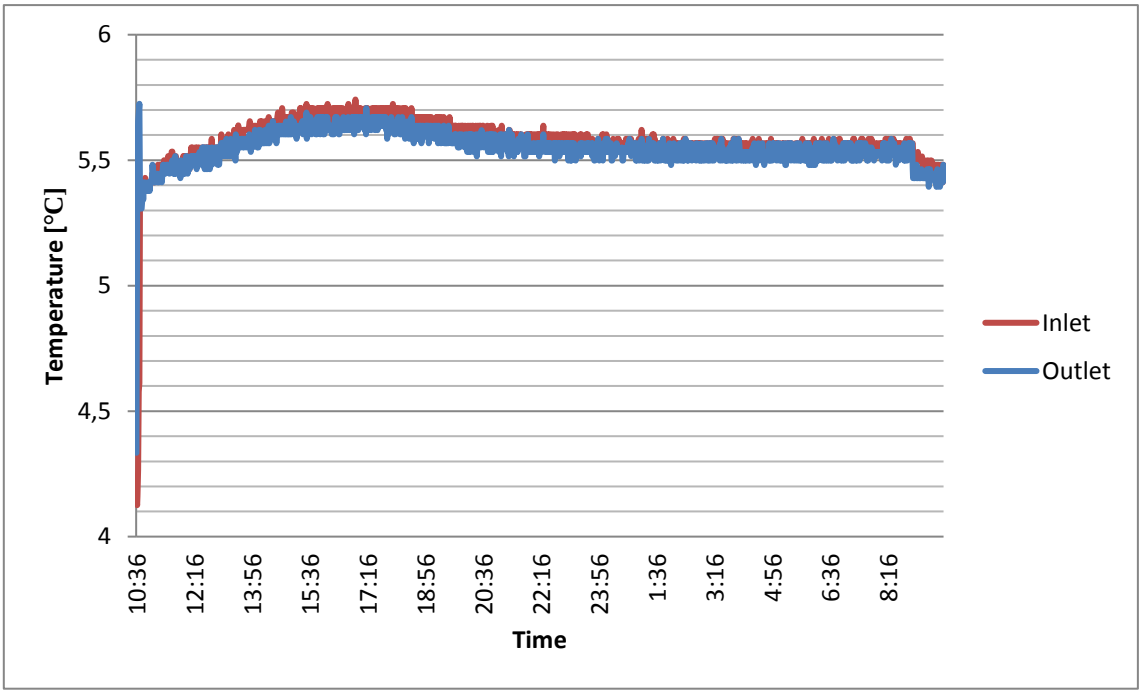

Figure 18. Initial ground temperature. The fluid is circulated without heating.

Even with the heater off, the pump gives out some heat. In addition, weather seems to have an effect, as is seen in the above graph.

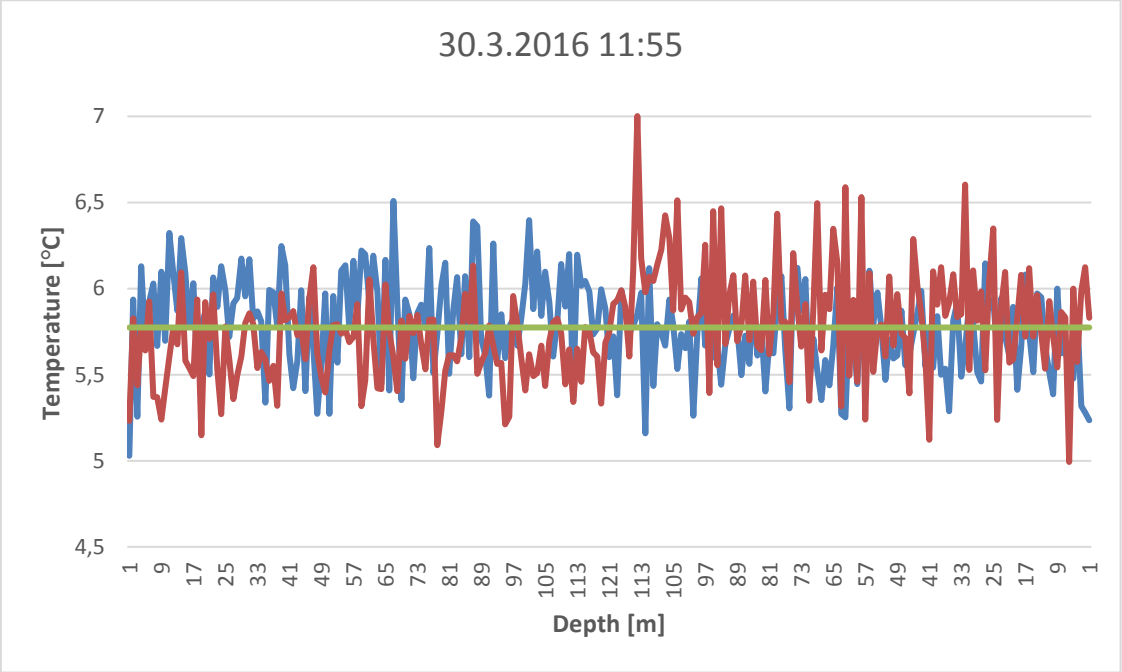

Figure 19. Undisturbed ground temperature with DTS.

Figure 19 illustrates the undisturbed ground temperature with depth distribution. There are two lines because of the double-ended measurement setup. Green line signifies the average value of 5,77 °C. This data represents readings at almost high noon, which does have an effect considering Figure 18. Geothermal gradient is not visible in figure 19, because DTS data was not logged prior to fluid circulation.

6.2. Thermal response test with heating only

A conventional TRT was performed prior to the bi-directional one. With it, thermal conductivity of the ground and borehole thermal resistance could be calculated. An accurate knowledge of these is valuable when designing large borehole heating systems with multiple BHEs.

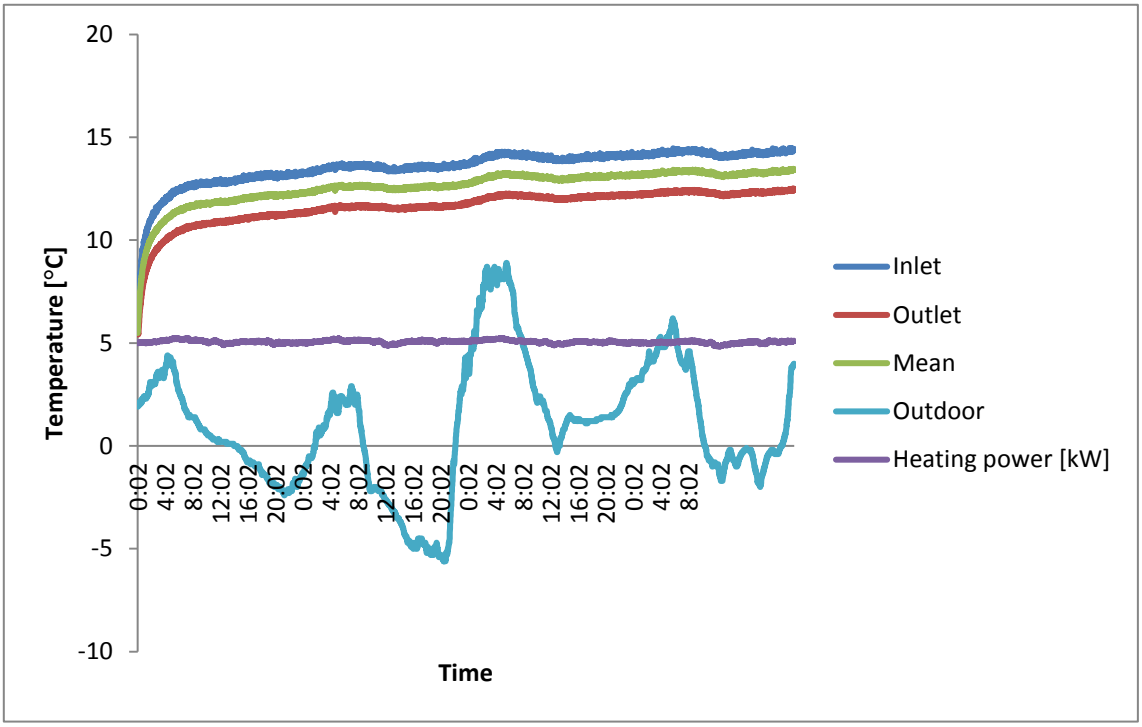

Figure 20. Four-day heating period.

As can be seen in Figure 20, weather conditions affected the results only marginally. This indicates that thermal insulation was performed satisfactorily. Outdoor temperature during the day was closer to the fluid temperature than during nights. Sunlight heating the surface of the tubes may also affect results somewhat.

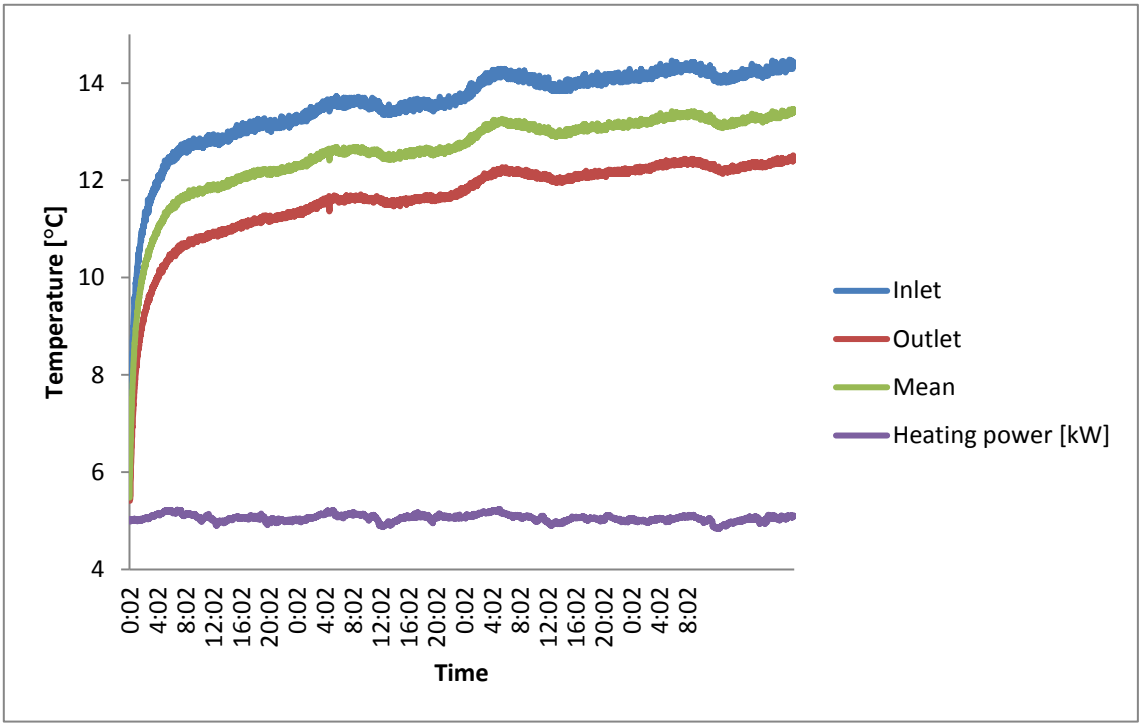

Figure 21. Four-day heating period with larger scale.

On a closer inspection, not only the weather, but also the miniscule heating power fluctuations seem to match with the peaks and valleys of the temperature curve (figure 21). Standard deviation of the electric heater input rate was calculated as 1,52 %. Maximum spike was 5,06 % of average power. ASHRAE recommends that to have an acceptable power quality, standard deviation must be equal to or smaller than 1,5 %, and maximum spike should be no larger than 10 % (Zhang et al. 2014: 855). Therefore, the power quality was considered a non-factor when analyzing the results.

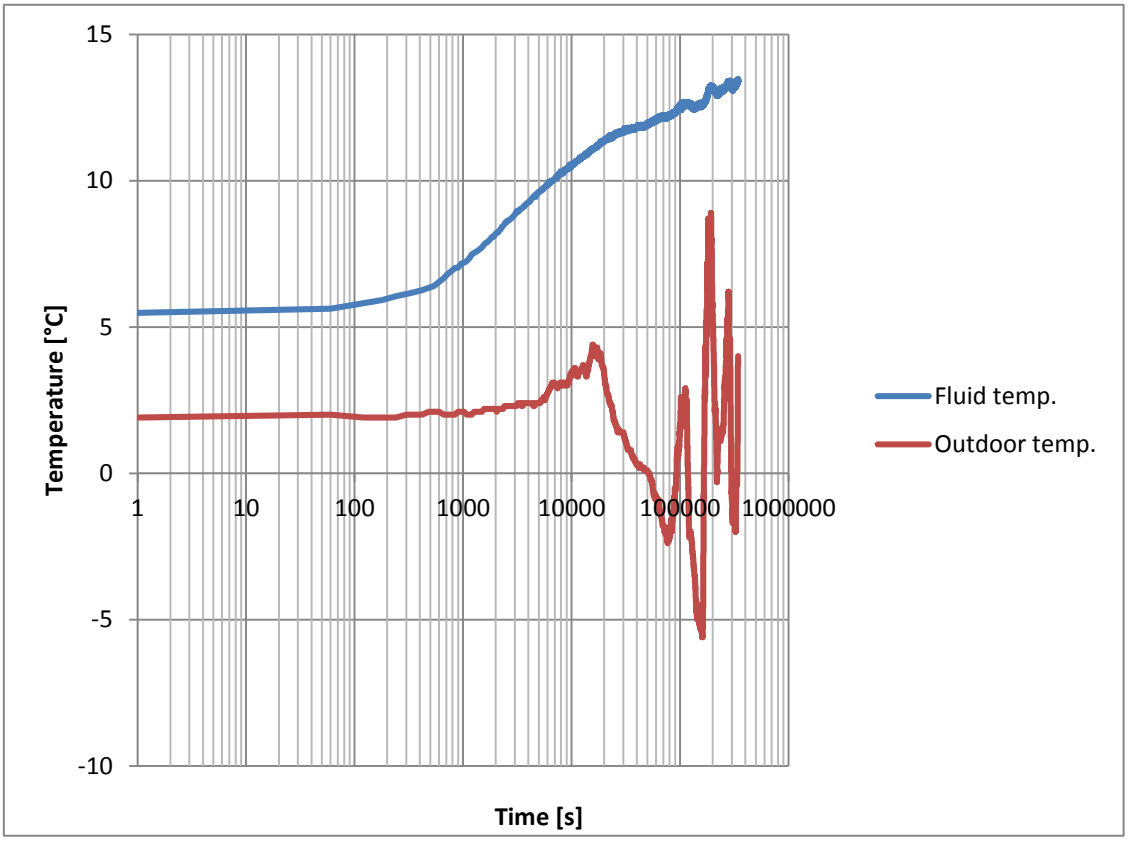

Figure 22. Outdoor and average fluid temperatures with logarithmic time during the heating.

Figure 22 shows mean fluid temperature on a logarithmic time scale. This is used in determining thermal conductivity of the ground, and thermal resistance between the borehole wall and the heat carrier fluid. A large portion of the early data is disregarded. The later, straighter part of the curve is linear approximated. The gradient and intercept of the line are used in calculation formulas.

The effect of outside temperature can also be seen on Figure 22. It does not make linearization much more difficult, which is more evident in Figure 23.

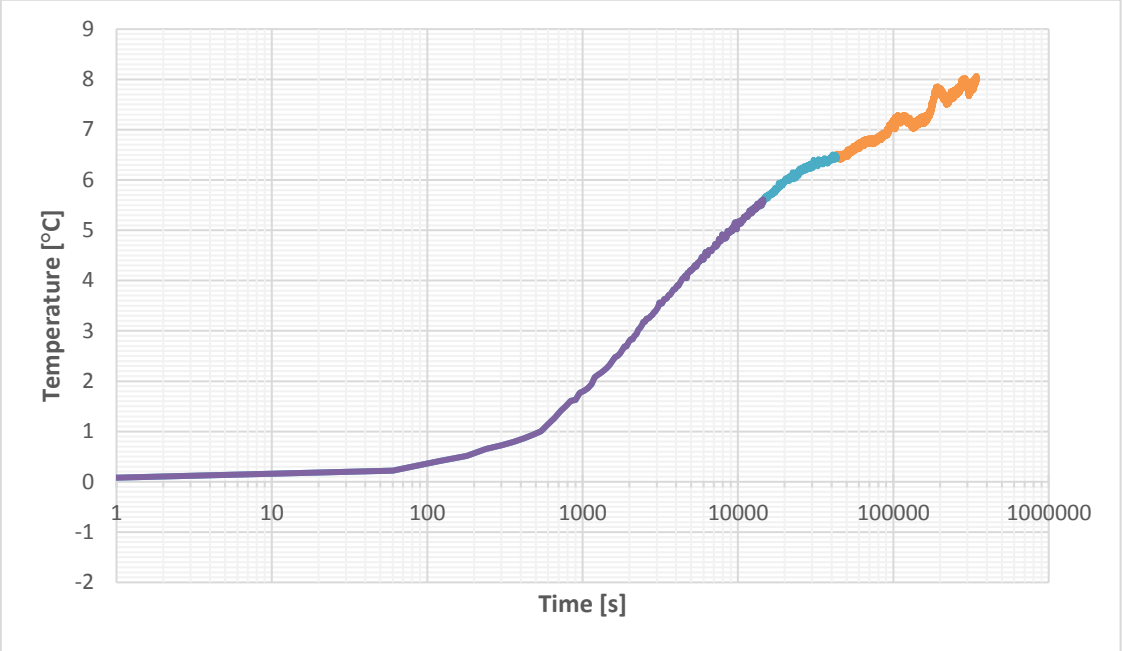

Figure 23. Mean fluid temperature with logarithmic time.

Figure 23 displays the starting point of the linear approximation. The undisturbed ground temperature 5,4 °C is already subtracted from the mean fluid temperature in the graph. The purple part of the line is ignored. If the first 12 hours are ignored, then only orange part is used (Spitler & Gehlin 2015: 1131). The point where purple turns to turquoise is the starting point as calculated with formula 5 (Banks 2008: 265),

$$t > 5 * r_b^{\,2} * \frac{S_{VC}}{\lambda}. \qquad (4)$$

r_b, borehole radius, m.

S_{VC}, approximated volume-specific heat capacity of the rock, J/(m^3*K).

λ, thermal conductivity of the rock, W/(m*K).

Formula 5

$$\lambda_{ef} = \frac{Q}{4\pi Hk} \quad (5)$$

is used to calculate the effective thermal conductivity.

Q, average thermal power, W.

H, depth of BHE, m.

k, the slope of Figure 22's linearization, K.

The formula was slightly modified by converting *k* from $\log_e$ to $\log_{10}$ time by multiplying with 2.303.

Effective thermal conductivity λ_{ef} was calculated as

$$\lambda_{ef} = \frac{5000\ W}{4\pi \times 122\ m \times 1{,}75\ K} = 4{,}29\ {}^{W}/_{m \times K} \quad (6)$$

with formula 5. Borehole thermal resistance R_b was determined as 0,07 with formula 7 and the resulting Figure 23. Both formulas are given by Gonet, Sliwa, Zlotkowski, Sapinska-Sliwa & Macuda 2012.

$$R_b = \frac{1}{q}(T_{av} - T_0) - \frac{1}{4\pi\lambda}\left[\ln\frac{4\alpha t}{r_0^2} + \frac{r_0^2}{4\alpha t} - \gamma\right] \quad (7)$$

q is *Q/H* from formula 5, 40,98 W/m.

T_{av}, average temperature of the heat carrier (measured variable), K.

$T_{0,}$ undisturbed ground temperature, 5,4 K.

λ, approximated thermal conductivity of the rock, 3,4 W/(m*K).

α, approximated thermal diffusivity of the rock, 1,679 x 10^{-6} m^2/s.

t, time (variable), s.

$r_{0,}$ borehole radius, 0,07 m.

γ, Euler constant, 0,5772.

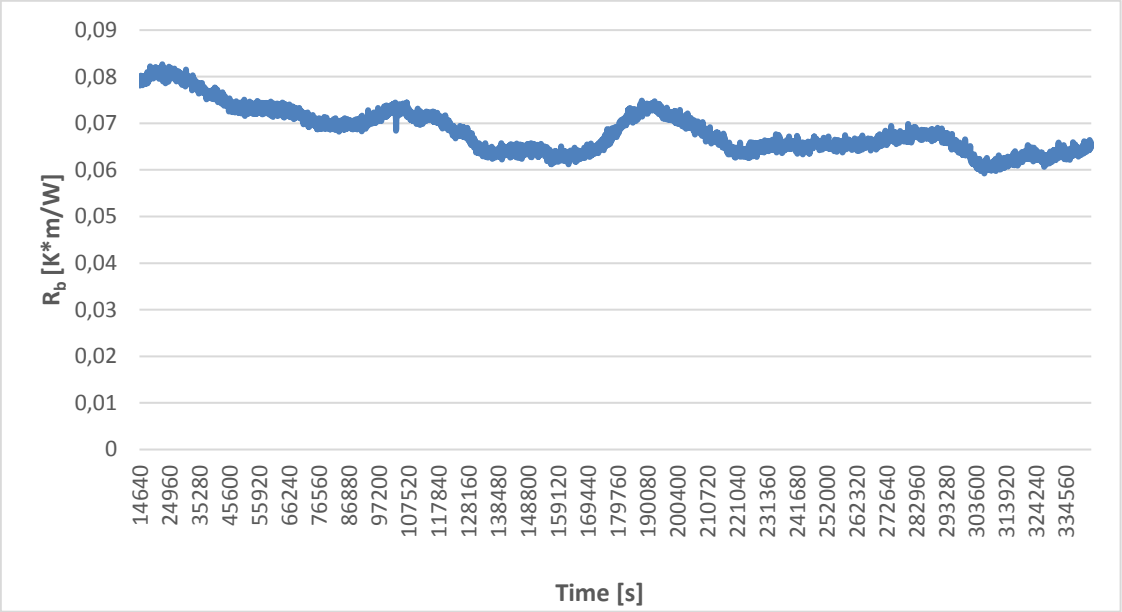

Figure 24. Borehole thermal resistance with time.

Figure 24 shows measured borehole thermal resistance with time. Values under 0,10 K*m/W may point towards advection or freezing in the borehole. This data was from a heating only test, which practically eliminates the possibility of freezing. Early data from Figure 24 was omitted by an amount determined by formula 4.

According to Rosén, Gabrielsson, Fallsvik, Hellström & Nilsson (2001: 137), water-filled boreholes tend to have a thermal resistance of 0,10 K*m/W. When they are frozen, that value tends to be 0,06 K*m/W. 0,03 K*m/W of that comes from the

polyethylene pipe. Temperature difference between the heat carrier and the borehole wall under normal operation with these values is usually about 2—4 °C.

Another source indicates that water-filled boreholes tend to have resistances similar to what was measured in this experiment. Namely 0,06—0,08 K*m/W for water-filled BHEs with heating and 0,09 K*m/W with ice. (Hellström 2011: 13.)

In conclusion, the borehole thermal resistance is in the range of what is expected. Thermal conductivity of the rock however seems rather high compared to values commonly attributed to granodiorite. The most probable explanation is that some amount of convection is taking place.

6.3. Heating and cooling test

The purpose of the heating and cooling test is to see how much the results from the heating and cooling phases differ from each other. A significant difference between them would be implicative of groundwater movement through the BHE. Temperature depth distribution data can be used to pinpoint the location of such flow. Heat storage efficiency can be calculated from the heating and cooling test.

Average heating and cooling power were 5,9 kW and 7,1 kW respectively. Heating periods were 17 h long. Cooling periods lasted for 7 h. When comparing the average temperatures of the heating and cooling phases to the initial ground temperature of 5,4 °C, the greater cooling power seems to produce a bigger difference (Figure 25). The thick parts in the graph represent a depth distribution of temperature.

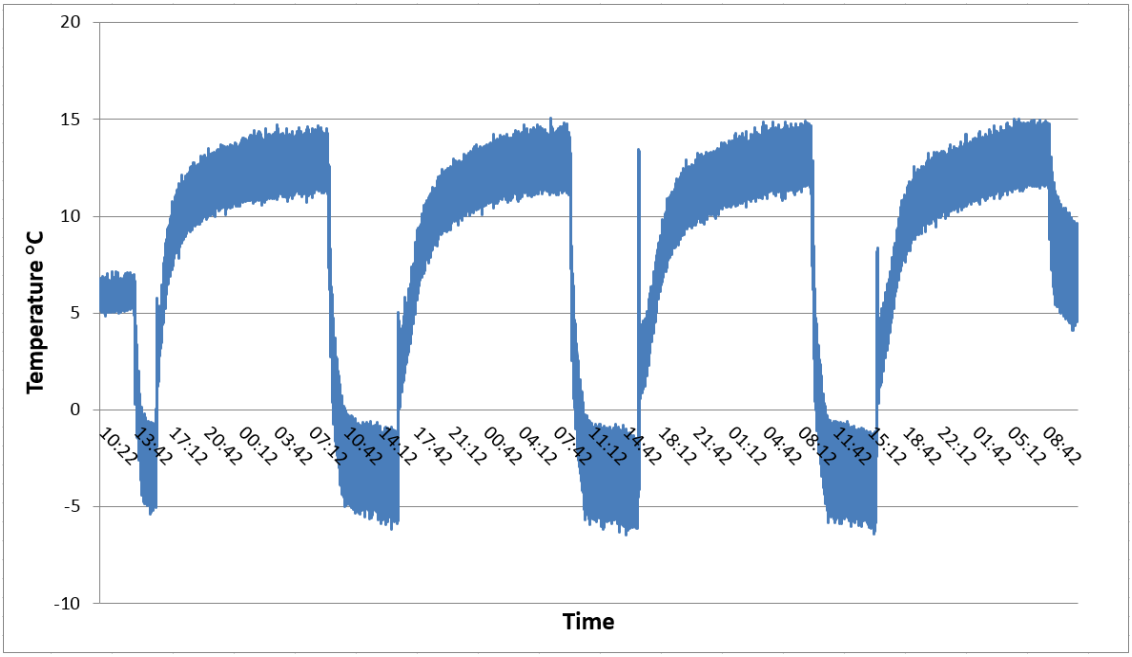

Figure 25. Overview of the heating and cooling test. The spikes are due to the activation of equipment. The thick parts represent values from top to bottom of the borehole at the same time.

It can be said that on a daily basis 5,9 kW * 17 h = 100,3 kWh was injected and 7,1 kW * 7 h = 49,7 kWh was extracted. The final heating period's peak temperature is some 1 K higher than that of the first. From this can be deduced that the storing efficiency of heat is somewhat higher than (49,7 kWh / 100,3 kWh) * 100% = 49,6 % on a time period of one day.

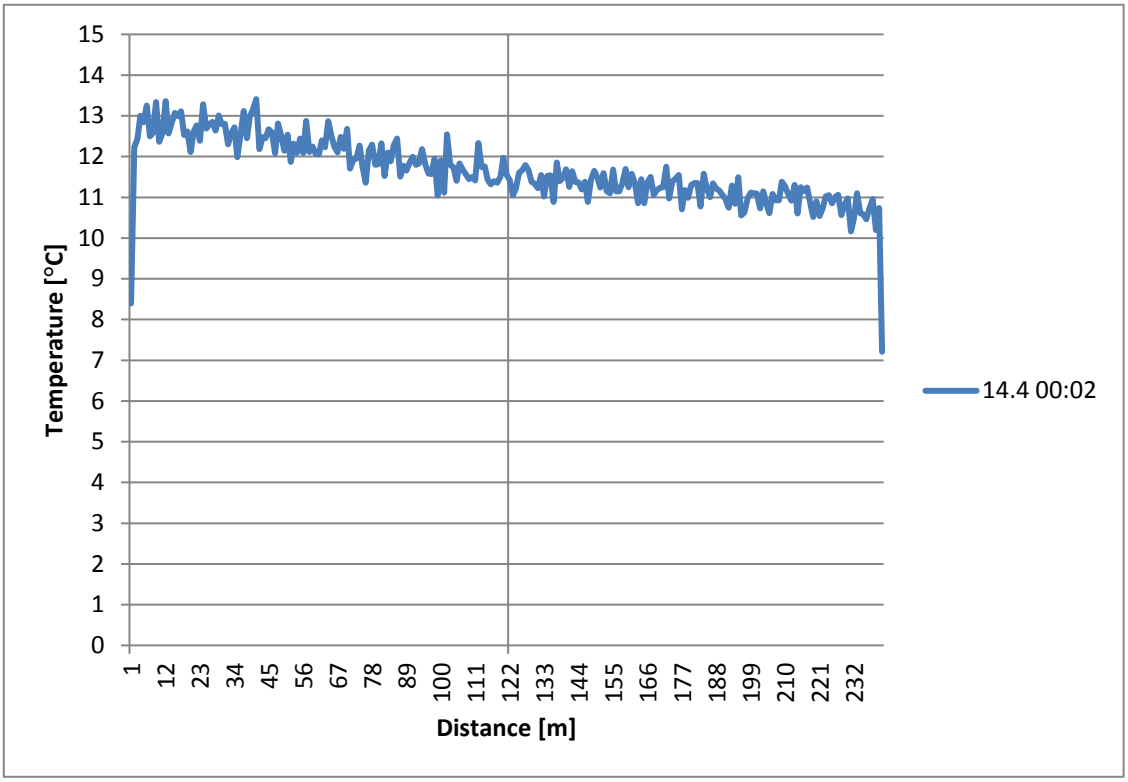

Figure 26. One meter below surface was still heavily affected by weather. These data points have been removed from other graphs.

Figure 26 shows DTS results from one point in time during a heating phase. The tube turns upwards at the 121-meter mark. Inlet temperatures are higher, because of the flow direction from the heater. Measurement accuracy is ±0,5 °C. The effect of weather seems to diminish rapidly with depth. At 2 meters deep, it is hardly noticeable.

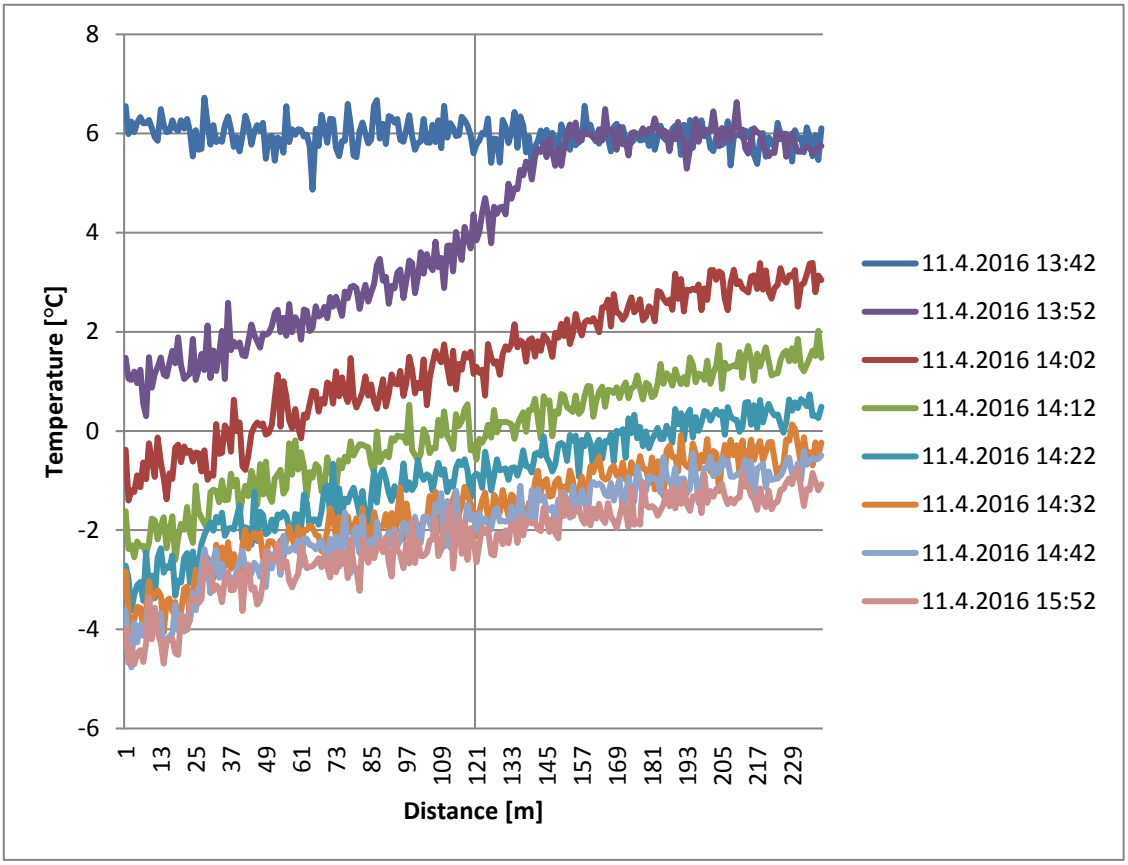

Figure 27. The first cooling phase.

The first cooling phase was shorter than the rest (Figure 27). After 1 h, the readings start to become harder to distinguish from each other. The purple line shows that it takes a while in the beginning for the cooling effect to catch up to the furthest reaches of the tube. The last line is one hour and ten minutes after the previous line. The rest are between ten-minute intervals.

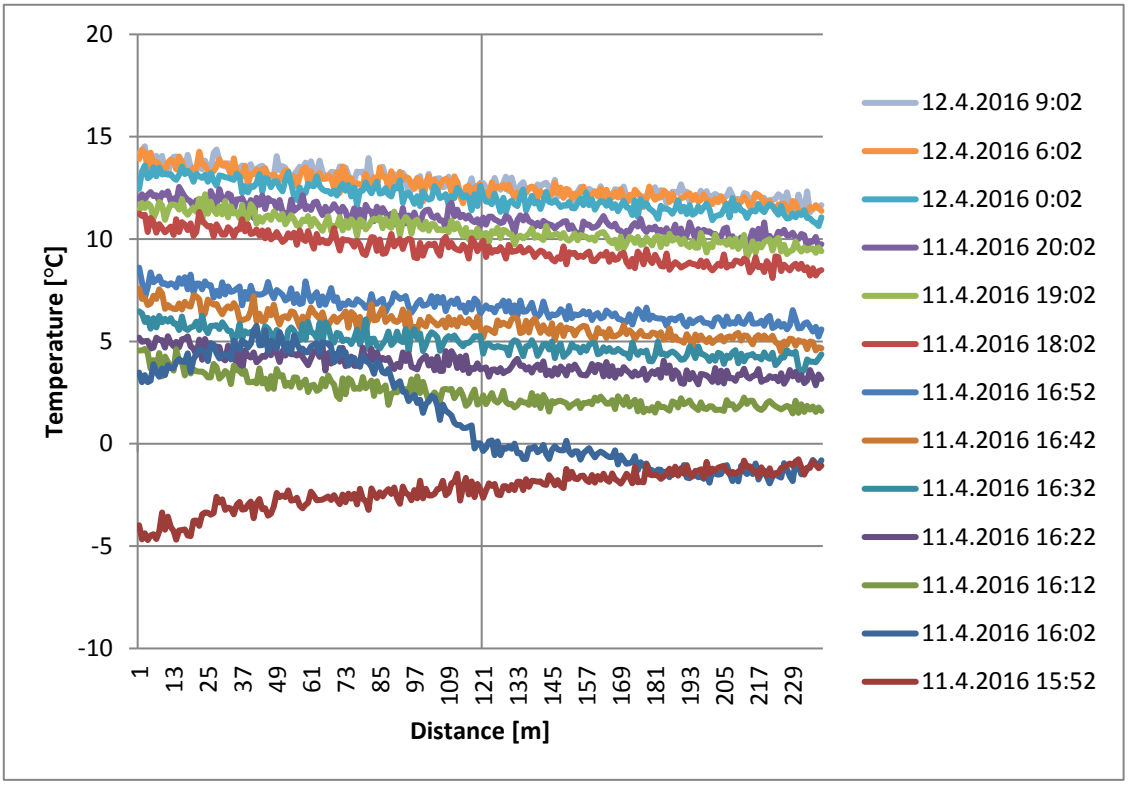

Figure 28. First night heating phase.

Figure 28 represents the first heating phase. The bottommost (red) line represents values just before activation of the resistor. It is the same as the bottommost line in the previous graph. The upper lines have more time between them, as can be seen from the legend.

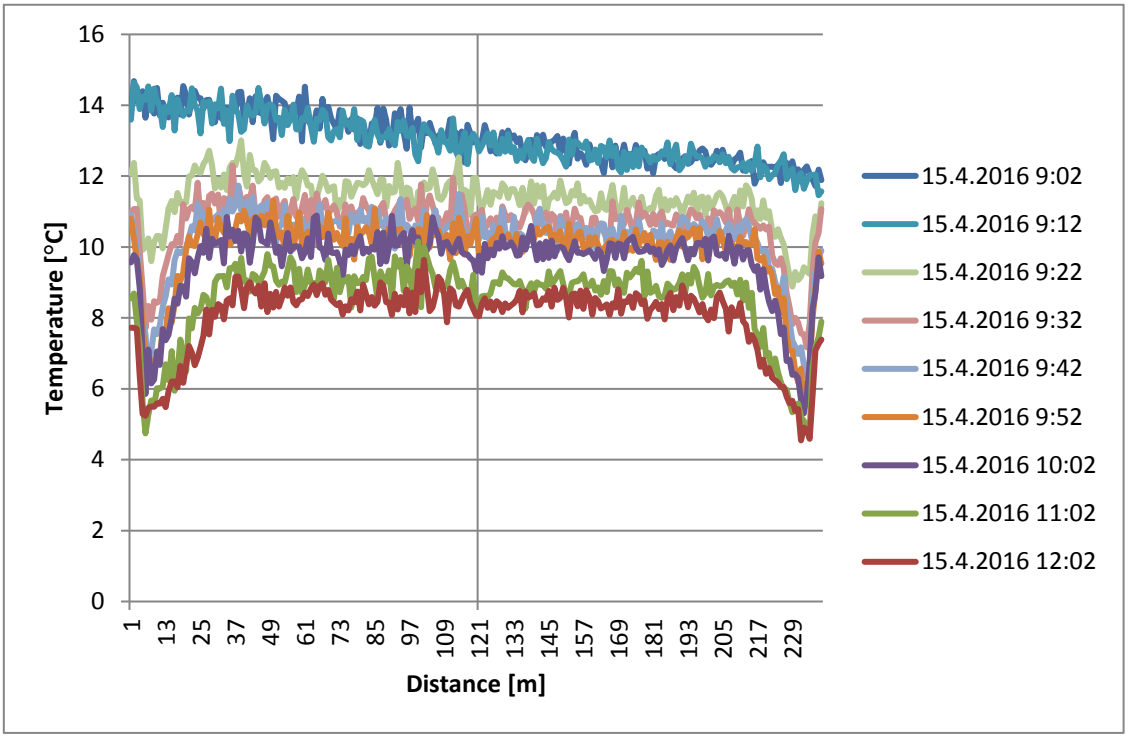

Figure 29. Final day of the experiment.

In Figure 29, the final heating phase ends and the fluid is allowed to settle without circulation. With the two first lines, the heater is still on. The temperature drops some 2 °C in 10 minutes and 5 °C in 3 hours depending on depth. Temperature drops more rapidly towards native temperature near the ground. This is probably due to weather effect, but could also be partially due to convection through the upper parts.

Regrettably, the cooling phases were too short to calculate conductivity accurately. Storage efficiency of heat could however be calculated to be around 50 % on a daily basis. No temperature anomalies were found, that would be indicative of water flow through fractures in the bedrock. Therefore, it can be concluded that groundwater flow through the BHE is mostly horizontal. Such flow is almost certainly located in the ground layer atop the rock. Temperature in the upper parts of the BHE is also affected by weather, making analysis more difficult.

CONCLUSION

A heating and cooling test with DTS was successfully performed with very little variation in power input. A heating only test gave a rather high average thermal conductivity for the rock. This suggests the presence of convective heat transfer. DTS on the other hand did not show any temperature anomalies the suggestive of fractures in the bedrock. First meter below the ground was heavily affected by weather. It can be inferred that the ground layer on top of the rock was thin and there was horizontal groundwater flow. Its effect was simply hard to distinguish from weather effect.

Heating should induce some vertical flow in the borehole. Still, closed water-filled boreholes without fractures should not have the kind of advection that is appropriate to treat as vertical – if it is thought of as a control volume.

Because the distributed temperature graphs did not show any anomalies, this test shall remain as reference for future experiments. From the heating and cooling test could however be calculated a heat storage efficiency of about 50% on a time scale of 24 hours.

In the future, when a longer cooling duration can be carried out, storage efficiency can be calculated more accurately. Moreover, a longer cooling phase will allow conductivity to be calculated from the cooling data also. Comparison between conductivity results from the heating and the cooling phase allows for an estimate on the magnitude of convective heat transfer.

REFERENCES

Acuña J. & B. Palm (2010). *A Novel Coaxial Borehole Heat Exchanger: Description and First Distributed Thermal Response Test Measurements*. Bali, Indonesia: Proceedings World Geothermal Congress.

Aittomäki A. (2001). *Lämpöpumppulämmitys*. Helsinki, Finland: Suomen lämpöpumppuyhdistys SULPU. 22 p.

Banks D. (2008). *An Introduction to Thermogeology. Ground Source Heating and Cooling*. Blackwell Publishing. ISBN 978-1-4051-7061-1.

BASIX 2016. *Ground source heat pump* [online]. [Cited 1 Nov. 2016]. Available from World Wide Web: <URL: https://www.basix.nsw.gov.au/iframe/energy-help/heating-and-cooling/ground-source-heat-pump.html>.

Claesson, J. & P. Eskilson (1987). *Conductive heat extraction by a deep borehole. Thermal analyses and dimensioning rules*. Lund, Sweden: Lund Institute of Technology.

Coleman T., B. Parker, C. Maldaner & M. Mondanos (2015). Groundwater flow characterization in a fractured bedrock aquifer using active DTS tests in sealed boreholes. *Journal of Hydrology* 528, 449–462.

Drake Landing Solar Community (2017). *Borehole Thermal Energy Storage (BTES)* [online]. [cited 10 Feb. 2017]. Available from World Wide Web: <URL: http://dlsc.ca/borehole.htm>.

Englund M., A. Mitrunen, P. Lehtiniemi & A. Ipatti (2008). *Kuituoptiset anturit siltarakenteiden mittauksissa*. Espoo, Finland: Fortum Power and Heat.

Gehlin S., G. Hellström & B. Nordell (2003). The influence of the thermosiphon effect on the thermal response test. *Renewable Energy* 28, 2239–2254.

Gonet A., T. Sliwa, A. Zlotkowski, A. Sapinska-Sliwa & J. Macuda (2012). *The Analysis of Expansion Thermal Response Test (TRT) for Borehole Heat Exchangers (BHE).* Stanford, California: Proceedings, Thirty-Seventh Workshop on Geothermal Reservoir Engineering.

Gustafsson A-M. (2006). *Thermal Response Test - Numerical simulations and analyses*. Luleå, Sweden: Luleå Univerity of Technology.

Hakala, P., A. Martinkauppi, I. Martinkauppi, N. Leppäharju & K. Korhonen (2014). *Evaluation of the Distributed Thermal Response Test (DTRT): Nupurinkartano as a case study*. Espoo, Finland: Geological survey of Finland.

Harris M. (2011). *Thermal Energy Storage in Sweden and Denmark. Potentials for Technology Transfer*. Lund, Sweden: IIIEE, Lund University.

Hellström G. (2011). *Advanced Thermal Response Testing and Its Relevance to Complex UTES Arrays* [presentation]. Neo Energy Sweden Ltd. Available from World Wide Web: <URL: http://www.gshp.org.uk/GroundSourceLive2011/GoranHellstrom_UTES_gsl.pdf>

Hellström G. (2012). *UTES Experiences from Sweden* [presentation]. Lund, Sweden: Lund University. Available from World Wide Web: <URL: http://www.icax.co.uk/pdf/REHAU_Hellstrom_UTES.pdf>

IEA ECES Annex 21 (2013), *Thermal Response Test (TRT).* Final Report.

IEA (2014). *Technology Roadmap. Energy storage*. Paris, France: IEA.

Kavanaugh S. (2000). *Field Tests for Ground Thermal Properties – Methods and Impact on Ground-Source Heat Pump Design*. ASHRAE Trans2000;106.

Leppäharju N. (2008). *Geophysical and geological factors in the utilization of ground heat*. Oulu, Finland: University of Oulu.

LIOS Technology (2015). *Distributed Temperature Sensing* [online]. [cited 5.4.2016]. Available in World Wide Web: <URL: http://www.lios-tech.com/Menu/Technology/Distributed+Temperature+Sensing>.

Mäkiranta A. (2013). *Distributed temperature sensing method – usability in asphalt and sediment heat energy measurements.* Vaasa, Finland: University of Vaasa.

Melinder Å. (2007). *Thermophysical Properties of Aqueous Solutions Used as Secondary Working Fluids*. Stockholm, Sweden: Royal Institute of Technology.

National Land Survey of Finland (2013). *Maankamara* [online]. [cited 1 Nov. 2016] Available from World Wide Web: <URL: http://gtkdata.gtk.fi/Maankamara/index.html>.

Nordell B. (1994). *Borehole Heat Store Design Optimization*. Luleå, Sweden: Luleå University of Technology.

Pinel P., C. Cruickshank, I. Beausoleil-Morrison & A. Wills (2011). A review of available methods for seasonal storage of solar thermal energy in residential applications. *Renewable and Sustainable Energy Reviews* 15, 3341– 3359.

Pirinen, P., H. Simola, J. Aalto, J-P. Kaukoranta, P. Karlsson & R. Ruuhela (2012). *Tilastoja suomen ilmastosta 1981-2010.* Helsinki: Finnish meteorological institute.

Powers J. (1997). *An introduction to fiber optic systems*. Second edition. United States of America: The McGraw-Hill Companies, Inc. ISBN 0-256-20414-4.

Quimby R. (2006). *Photonics and Lasers – an Introduction*. New Jersey: John Wiley & Sons, Inc.

Rakennustutkimus RTS Oy (2016). *Maalämpö jo joka toiseen uuteen omakotitaloon* [online]. Updated 15 Aug. 2016 [cited 17 May 2017]. Available from World Wide Web: <URL: http://www.suomirakentaa.fi/omakotirakentaja/laemmitys/maalampo>.

Rantamäki M., R. Jääskeläinen & M. Tammirinne (2006). *Geotekniikka*. Helsinki: Otatieto.

Reuss M., M. Beck & J. P. Müller (1997). Design of a Seasonal Thermal Energy Storage in the Ground. *Solar Energy* 59, 247—257.

Rosén B., A. Gabrielsson, J. Fallsvik, G. Hellström & G. Nilsson (2001). *System för värme och kyla ur mark- En nulägesbeskrivning*. Linköping, Sweden: Swedish Geotechnical Institute.

Rototec (2016). *Referenssikartta maalämpöprojekteistamme* [online]. [cited 2 Nov. 2016] Available from World Wide Web: <URL: http://www.geodrill.fi/referenssikartta/>.

Sanner B., G. Hellström, J. Spitler & S. Gehlin (2005). *Thermal Response Test – Current Status and World-Wide Application*. Antalya, Turkey: Proceedings World Geothermal Congress.

Scorpo A., B. Nordell & S. Gehlin (2016). *A Method to Estimate the Hydraulic Conductivity of the Ground by TRT Analysis*. National Ground Water Association.

Sensornet (2007). *Oryx DTS User Manual v4*. London, United Kingdom: Sensornet Ltd.

Seppänen O. (2001). *Rakennusten lämmitys*. Helsinki: Suomen LVI-liitto ry.

Signorelli S., S. Bassetti, D. Pahud & T. Kohl (2007). Numerical evaluation of thermal response tests. *Geothermics* 36, 141–166.

Smolen J. & A. van der Spek (2003). *Distributed Temperature Sensing. A DTS Primer for Oil & Gas Production.* Hague, Netherlands: Shell International Exploration and Production B.V.

Spitler J. & S. Gehlin (2015). Thermal response testing for ground source heat pump systems—An historical review. *Renewable and Sustainable Energy Reviews* 50, 1125–1137.

Syrjälä T. (2013). *Geoenergialähteen termisten ominaisuuksien mittaamiseen soveltuvan laitteiston suunnittelu ja toteutus*. Vaasa: University of Vaasa, Faculty of Technology.

Official Statistics of Finland (2015). *Energy consumption in households* [online]. Helsinki: Statistics Finland, Updated 20 Nov. 2015 [cited 17 May 2017]. Available from World Wide Web: <URL: http://www.stat.fi/til/asen/2014/asen_2014_2015-11-20_tie_001_fi.html>. ISSN 2323-329X.

Wagner V., P. Blum, M. Kübert & P. Bayer (2013). Analytical approach to groundwater-influenced thermal response tests of grouted borehole heat exchangers. *Geothermics* 46, 22–31.

Witte H. (2001). *Geothermal Response Tests with Heat Extraction and Heat Injection: Examples of Application in Research and Design of Geothermal Ground Heat Exchangers*. Lausanne: EPFL.

Zhang C., Z. Guo, Y. Liu, X. Cong & D. Peng (2014). A review on thermal response test of ground-coupled heat pump systems. *Renewable and Sustainable Energy Reviews* 40, 851–867.